Synthesis, Characterization, and Reactivity of New Clusters That Contain the $[MFe_3S_4]^0$ Core, M = Mo, W. A Weakly Perturbed $[MFe_3S_4]^0$ Unit Structurally and Electronically Analogous to the Reduced Three-Iron Centers in Ferredoxins

D. Coucouvanis,*[1] Saleem A. Al-Ahmad,[1] A. Salifoglou,[1] V. Papaefthymiou,[2] A. Kostikas,[3] and A. Simopoulos[3]

Contribution from the Department of Chemistry, The University of Michigan, Ann Arbor, Michigan, 48109-1055, the Department of Physics, University of Ioannina, Ioannina, Greece, and the National Center for Scientific Research Demokritos, Aghia Paraskevi Attiki, Greece.
Received September 3, 1991

Abstract: The synthesis, characterization, and reactions of the new "cubane"-type clusters $(Et_4N)_3[Fe_3S_4L_3M(CO)_3]$, M = Mo, L = EtS^-, BzS^-, *p*-$OMePhS^-$, PhO^-, Cl^-; M = W, L = *p*-$OMePhS^-$, are described in detail. These clusters are obtained in a good yield as $(Et_4N)^+$ salts, by the reaction of the $[Fe_3S_4L_4]^{3-}$ linear trimer with $M(CO)_3(MeCN)_3$, M = Mo, W. The $(Et_4N)_3[Fe_3S_4(EtS)_3Mo(CO)_3]\cdot CH_3CN$ cluster crystallizes in the *Pbcm* space group with cell dimension a = 16.557 Å, b = 18.915 Å, c = 17.110 Å; $\alpha = \beta = \gamma = 90°$, z = 4. Intensity data were collected using a four-circle computer-controlled diffractometer. Refinement of 198 parameters on 1290 data, ($F_o^2 > 3\sigma(F_o^2)$), converged to a final R_w value of 0.065. The structure of the cubic $[Fe_3S_4Mo]^0$ core shows the $Mo(CO)_3$ fragment interacting weakly with the Fe_3S_4 ligand with a Mo–S bond length of 2.63 (1) Å and a Fe–Mo distance of 3.274 (5) Å. Electrochemical measurements on the $[Fe_3S_4L_3M(CO)_3]^{3-}$ complexes in CH_2Cl_2 show two reversible reduction waves that are assigned for the $2^-/3^-$ and $3^-/4^-$ redox couples. The ^1H NMR spectra of the complexes exhibit isotropically shifted resonances. The Moessbauer spectra of the complexes show broad doublets. The zero field spectra of $(Et_4N)_3[Fe_3S_4(EtS)_3M(CO)_3]$ and $(Et_4N)_3[Fe_3S_4(BzS)_3M(CO)_3]$ at 4.2 K show structure and can be fit with two or three component doublets in a 2:1 or 1:1:1 ratios. The magnetically perturbed spectra, recorded in an applied field of 4.0 and 6.0 T, can be interpreted in terms of a model where a ferromagnetically coupled ($S_{1,2} = {}^9/_2$) Fe^{2+}/Fe^{3+} pair couples antiferromagnetically with the $S = {}^5/_2$ Fe^{3+} site to give an S = 2 ground state. The fine and hyperfine parameters, obtained by simulations of the Moessbauer spectra, are remarkably similar to parameters reported previously for the Fe_3S_4 centers in *Desulfovibrio gigas* Fd II and aconitase. The oxidative decarbonylation reactions of the $(Et_4N)_3[Fe_3S_4L_3Mo(CO)_3]$ with quinone afford the solvated single cubane $(Et_4N)_2[Fe_3S_4Cl_3Mo(MeCN)(cat)]$ when the terminal ligand on the iron site is Cl^-, and the doubly-bridged double-cubane $(Et_4N)_4[Fe_3S_4(EtS)_3Mo(cat)]_2$ when the terminal ligand is EtS^-. The reaction of $(Et_4N)_3[Fe_3S_4(EtS)_3Mo(CO)_3]$ with diethyl disulfide afforded the triply-bridged double-cubane cluster $(Et_4N)_3[Fe_6S_8(EtS)_9Mo_2]$ in moderate yield. Upon heating in solution the $(Et_4N)_3[Fe_3S_4L_3Mo(CO)_3]$ clusters (L = Cl^-, *p*-$COMePhO^-$) are converted to the corresponding, prismane–adduct, octanuclear clusters $(Et_4N)_4[Fe_6S_6(L)_9[Mo(CO)_3]_2]$. In CH_3CN solution the $Mo(CO)_3$ fragment in the $[Fe_3S_4(EtS)_3Mo(CO)_3]^{3-}$ cluster can be replaced by $FeCl^+$. In this reaction a statistical mixture of $[Fe_4S_4(Cl)_x(EtS)_{4-x}]^{2-}$ clusters is obtained, as indicated by ^1H NMR spectroscopy.

Introduction

The redox properties of a great number of non-heme iron sulfur proteins, ferredoxins, are based on Fe/S clusters that contain either cubic $[Fe_4S_4]^{1+,2+}$ or planar, rhombic, $[Fe_2S_2]^{2+}$ central cores.[4] A smaller class of ferredoxins, that include ferredoxin I from *Azotobacter vinelandii*, ferredoxin II from *Desulfovibrio gigas*, and aconitase, contain Fe/S centers with the unusual $[Fe_3S_4]^+$ core.[5] On the basis of EXAFS analyses,[6] a cubane type of structure was suggested for the $[Fe_3S_4]^+$ core. Later this suggestion was verified by single crystal X-ray crystallographic studies on Fd I from *A. vinelandii*[7] and more recently on Fd II from *D. gigas*.[8] In both determinations the structure of the $[Fe_3S_4]^+$ core is found with a configuration similar to that of the Fe_4S_4 "cubanes"[9] but lacks one Fe atom and contains three, rather than four, terminal cysteinyl ligands. Chemical oxidation[10] of the Fe_4S_4 centers in certain ferredoxins leads to the formation of Fe_3S_4 centers that can be reconverted to Fe_4S_4 upon addition of Fe. The $CoFe_3S_4$[11] and $ZnFe_3S_4$[12] cubane derivatives of the Fe_3S_4 center in *D. gigas* ferredoxin II (Fd II) are obtained by the addition of Co^{2+} or Zn^{2+} to dithionite reduced Fd II. The "oxidized" form of the $CoFe_3S_4$ derivative formally contains $Co^{II}Fe^{II}[Fe^{III}]_2$ and shows Moessbauer parameters and EPR spectra consistent with a $S = {}^1/_2$ ground state.

Synthetic analogues for the ferredoxin Fe_4S_4 and Fe_2S_2 centers are available in a large number of completely characterized Fe/S clusters.[13] In contrast, an *unsupported structural analogue* for the Fe_3S_4 center is not as yet available, although tightly bound Fe_3S_4 structural subunits are present in the structurally congruent VFe_3S_4,[14] $MoFe_3S_4$,[15] and $ReFe_3S_4$[16] single cubes.

(1) The University of Michigan.
(2) The University of Ioannina.
(3) National Center for Scientific Research Demokritos.
(4) *Iron–Sulfur Proteins*; Lovenberg, W., Ed.; Academic Press: New York, 1977; Vols. 1–3.
(5) Beinert, H.; Thomson, A. J. *Arch. Biochem. Biophys.* **1984**, *222*, 333–361.
(6) (a) Antonio, M, R.; Averill, B. A.; Moura, I.; Moura, J. J.; Orme-Johnson, W. H.; Teo, B. K.; Xavier, A. V. *J. Biol. Chem.* **1982**, *257*, 6646. (b) Beinert, H.; Emptage, M. H.; Dreyer, J.-L.; Scott, R. A.; Hahn, J. E.; Hodgson, K. O.; Thomson, A. J. *Proc. Natl. Acad. Sci. U.S.A.* **1983**, *80*, 393.
(7) Stout, G. H.; Turley, S.; Sieker, L. C.; Jensen, L. H. *Proc. Natl. Acad. Sci. U.S.A.* **1988**, *85*, 1020–1022.
(8) Kissinger, C. R.; Adman, E. T.; Sieker, L. C.; Jensen, L. H. *J. Am. Chem. Soc.* **1988**, *110*, 8721–8723.
(9) Carter, C. W., Jr. In *Iron–Sulfur Proteins*; Lovenberg, W., Ed.; Academic Press: New York, 1977; Vol. 3, pp 157–204.
(10) (a) Thomson, A. J.; Robinson, A. E.; Johnson, M. K.; Cammack, R.; Rao, K. K.; Hall, D. O. *Biochim. Biophys. Acta* **1981**, *637*, 423. (b) Ackrell, B. A. C.; Kearney, E. B.; Mims, W. B.; Peisach, J.; Beinert, H. *J. Biol. Chem.* **1984**, *259*, 4015.
(11) Moura, I.; Moura, J. J. G.; Munck, E.; Papaefthymiou, V.; LeGall, J. *J. Am. Chem. Soc.* **1986**, *108*, 349.
(12) Surerus, K. K.; Munck, E.; Moura, I.; Moura, J. J. G.; LeGall, J. *J. Am. Chem. Soc.* **1987**, *109*, 3805.
(13) (a) Berg, J. M.; Holm, R. H. In *Iron–Sulfur Proteins*; Spiro, T. G., Ed.; Wiley-Interscience: New York, 1982; Chapter 1. (b) Holm, R. H.; Ibers, J. A. In *Iron–Sulfur Proteins*; Lovenberg, W., Ed.; Academic Press: New York, 1977; Vol. 3, Chapter 7.
(14) (a) Kovacs, J. A.; Holm, R. H. *J. Am. Chem. Soc.* **1986**, *108*, 340. (b) Kovacs, J. A.; Holm, R. H. *Inorg. Chem.* **1987**, *26*, 702.

0002-7863/92/1514-2472$03.00/0

The chemical oxidation of synthetic cubanes, that contain the $Fe_4S_4^{2+}$ cores, does not lead to the synthesis of analogues for the Fe_3S_4 centers, and the results of such oxidations depend greatly on the nature of the terminal ligands. In a previous report we have shown[17] that the irreversible oxidation of the $[Fe_4S_4Cl_4]^{2-}$ cubane leads, in high yield, to the $[Fe_6S_6Cl_6]^{2-}$ oxidized prismane. At a later date it was demonstrated[18] that a stable oxidized cubane that contained the $[Fe_4S_4]^{3+}$ core in fact could be obtained by chemical oxidation of the $[Fe_4S_4(SR)_4]^{2-}$ cubane (R = 2,4,6-*i*-$Pr_3C_6H_2$). The importance of the steric characteristics of the terminal ligands in the outcome of the chemical oxidation of the synthetic Fe_4S_4 clusters becomes apparent in the oxidation of the $[Fe_4S_4(S\text{-}t\text{-}Bu)_4]^{2-}$ cubane with $Fe(CN)_6^{3-}$. This reaction is reported[19] to give a new unstable species that at −40 °C displays spectroscopic characteristics similar to those of the Fe_3S_4 centers in the 3Fe proteins. A heteronuclear cubane cluster, apparently similar to the *D. gigas* $CoFe_3S_4$ derivative center, forms by the "controlled aerobic oxidation" of the $[Fe_4S_4(SR)_4]^{2-}$ cubane (R = 2,4,6-*i*-$Pr_3C_6H_2$) in the presence of $CoCl_2$ and has been reported[20] to contain a $[CoFe_3S_4]^{2+}$ core with a $S = {}^1/_2$ ground state.

Recently, we reported[21] on a weak complex of $Mo(CO)_3$ with the $[Fe_3S_4(SEt)_3]^{3-}$ "ligand". The magnetically coupled, $[Fe_3S_4(SEt)_3Mo(CO)_3]^{3-}$ cluster (with an integer spin ground state) contains the $[Fe_3S_4]^0$ subunit that may be the least perturbed structural analogue for the $[Fe_3S_4]^0$ center in the reduced form of the 3Fe ferredoxins. This cluster is obtained readily by the reaction of $Mo(CO)_3(CH_3CN)_3$ with the $Fe_3S_4(SEt)_4]^{3-}$ linear trimer[22] (eq 1). Recently, a "spin-isolated" $[Fe_3S_4]^0$ subunit in

$$[Fe_3S_4(SEt)_4]^{3-} + Mo(CO)_3(CH_3CN)_3 \rightarrow [Fe_3S_4(SEt)_3Mo(CO)_3]^{3-} + {}^1/_2EtSSEt \quad (1)$$

a $S = 2$ state has been identified by Moessbauer spectroscopic analysis of the site-differentiated $[Fe_4S_4(LS_3)(t\text{-}BuNC)_3]^-$ cubane. This subunit, that is bound to a low spin $Fe^{II}(t\text{-}BuNC)_3$ fragment, is electronically very similar to the singly reduced 3Fe site in the 3Fe ferredoxins.[23]

Subsequent to our original communication on the synthesis of $[Fe_3S_4(SEt)_3Mo(CO)_3]^{3-}$, two reports have appeared in the literature that describe the synthesis of clusters with the $[NiFe_3S_4]^0$ and $[CoFe_3S_4]^{2+}$ cores from the reaction of the $[Fe_3S_4(SEt)_4]^{3-}$ linear trimer with either $(Ph_3P)_4Ni$[24] or $CoCl_2$.[20] These reports suggest that the reaction depicted in eq 1 is a general one and that the synthesis of the heteronuclear MFe_3S_4 cubanes involves the metal (Mo, Co, Ni) promoted intramolecular oxidation of one of the EtS^- terminal ligands in the $[Fe_3S_4(SEt)_4]^{3-}$ complex followed by a structural rearrangement of the resultant $[Fe_3S_4(SEt)_3]^{3-}$ unit.

In this paper we report in detail on the crystal structure of the $[Fe_3S_4(SEt)_3Mo(CO)_3]^{3-}$ anion, the synthesis, electronic structures, and chemical reactions of the new $[Fe_3S_4(L)_3M(CO)_3]^{3-}$ clusters (M = Mo, W) and a detailed analysis of the Moessbauer spectra of the $[Fe_3S_4(L)_3Mo(CO)_3]^{3-}$ clusters (L = EtS^-, BzS^-), which shows that the $[Fe_3S_4]^0$ units in these compounds have an electronic ground state nearly identical to the same unit in the singly reduced 3Fe site in the 3Fe ferredoxins.

Experimental Section

All complexes were prepared in an inert atmosphere using a Vacuum Atmosphere Dri-Lab glovebox filled with prepurified (Matheson) dinitrogen gas.

Acetonitrile was distilled from calcium hydride under nitrogen. Tetrahydrofuran and diethyl ether were distilled over sodium benzophenone. Thiophenol, ethanethiol, *p*-(methoxythio)phenol, benzylthiol, and benzoyl chloride were purchased from Aldrich Chemical Company and used without further purification. Molybdenum hexacarbonyl, tungsten hexacarbonyl, and anhydrous iron(II) chloride were purchased from Alfa and were used as purchased. $Mo(CO)_3(CH_3CN)_3$ and $W(CO)_3(CH_3CN)_3$ were prepared as described in the literature.[25] The sodium salt of ethanethiol was made by reacting ethanethiol with sodium metal in ethanol under a dinitrogen atmosphere. The $(Et_4N)_3Fe_3S_4(SEt)_4$ cluster was made according to a modified literature method.[22a]

Elemental analyses were carried out by Oneida Research Services Inc., Whitesboro, NY and by the analytical services laboratory in the chemistry department at the University of Michigan.

Physical Methods. Visible and ultraviolet spectra were recorded on a Varian Cary 219 spectrophotometer using a 1-mm path length quartz cell. Proton NMR spectra were obtained on a Bruker 300 MHz pulse, Fourier transform NMR spectrometer. Tetramethylsilane (Me_4Si) was used as an internal standard. Chemical shifts are reported in parts per million. The following convention is used whenever isotropically shifted spectra are reported: A positive sign is assigned to resonances appearing downfield from TMS, and a negative sign is assigned to resonances appearing upfield from TMS. Cyclic voltammetric measurements were performed on a Princeton Applied Research Model 175 Universal programmer. The electrochemical cell used had platinum working and auxiliary electrodes. As reference electrode, a saturated calomel electrode was used. All solvents used in the electrochemical measurements were properly dried and distilled. The supporting electrolyte used was *tetra-n*-butylammonium perchlorate $(C_4H_9)_4NClO_4$. Normal concentrations used were 0.001 M in electroanalyte and 0.1 M in supporting electrolyte. Purified argon was used to purge the solutions prior to the electrochemical measurements. The Moessbauer spectra were obtained from 4.2 K to room temperature with a constant acceleration spectrometer. The source was 100 mCi of ^{57}Co in a Rh matrix and was held at room temperature.

Preparation of Compounds. Tris(tetraethylammonium) Tetrakis(ethanethiolato)tris(μ_3-sulfido)triferrate(3III), $(Et_4N)_3[Fe_3S_4(EtS)_4]$. A mixture of $FeCl_2$ (2.0 g, 15.7 mmol), Et_4NCl (5.15 g, 31.4 mmol), and NaSEt (5.25 g, 62.8 mmol) was stirred in acetonitrile, CH_3CN, for 45 min. The mixture was filtered, and the solid (mainly NaCl) was washed several times with CH_3CN. The washings and the filtrate were combined, and the solvent was removed under vacuum. The residue was dissolved in 100 mL of acetone, and 0.64 g (20 mmol) of sulfur was added with stirring. After stirring for several hours a microcrystalline solid formed. The mixture was allowed to stir for an additional 8 h. After that period of time, the solid was collected by filtration and washed several times with acetone. The yield was 3.70 g (70%). The spectroscopic properties of the product were identical to those reported previously[22a] and confirm its identity as $(Et_4N)_3[Fe_3S_4(EtS)_4]$.

Tris(tetraethylammonium) Tris(ethanethiolato)tris(μ_3-sulfido)triferrate(II,2III)-Molybdenum(0) Tricarbonyl Acetonitrile Solvate, $(Et_4N)_3[Fe_3S_4(EtS)_3Mo(CO)_3]\cdot CH_3CN$ (I). To a solution of 1.5 g (1.6 mmol) of $(Et_4N)_3[Fe_3S_4(EtS)_4]$ in 30 mL of CH_3CN was added 0.5 g (1.65 mmol) of $Mo(CO)_3(CH_3CN)_3$, and the solution was stirred for 25 minutes at room temperature. The solution was then filtered, and to the filtrate were added 75 mL of THF and 100 mL of ether. Upon standing overnight, a crystalline solid formed. The product was collected by filtration, washed with ether, and dried in vacuum: yield 1.1 g (60%). Anal. Calcd for $C_{37}H_{78}N_4O_3Fe_3S_4Mo$ (MW = 1091.8): C, 38.5; H, 7.22; N, 5.13; S, 20.56; Fe, 15.35; Mo, 8.79. Found: C, 38.06; H, 6.8; N, 4.73; S, 19.73; Fe, 15.16; Mo, 8.57.

Tris(tetraethylammonium) Tris(benzylthiolato)tris(μ_3-sulfido)triferrate(II,2III)-Molybdenum(0) Tricarbonyl, $(Et_4N)_3Fe_3S_4(SCH_2C_6H_5)_3Mo(CO)_3$ (II). To a solution of 1.0 g (1.08 mmol) of $(Et_4N)_3Fe_3S_4(SEt)_4$ in 30 mL of CH_3CN was added 2 mL (9.4 mmol) of $HSCH_2C_6H_5$ with stirring. After stirring for 1 h the color changed to brown-purple. The solution was then filtered, and the solvent was removed to dryness. The residue was washed several times with ether and then dissolved in 30 mL of CH_3CN. To the resulting solution was

(15) Holm, R. H.; Simhon, E. D. In *Molybdenum Enzymes*; Spiro, T. G., Ed.; Wiley-Interscience: New York, 1985; pp 1–87.
(16) Ciurli, S.; Carney, M. J.; Holm, R. H.; Papaefthymiou, G. C. *Inorg. Chem.* **1989**, *28*, 2696.
(17) Coucouvanis, D.; Kanatzidis, M. G.; Dunham, W. R.; Hagen, W. R. *J. Am. Chem. Soc.* **1984**, *106*, 7998.
(18) (a) O'Sullivan, T.; Millar, M. M. *J. Am. Chem. Soc.* **1985**, *107*, 4096. (b) Papaefthymiou, V.; Millar, M. M.; Munck, E. *Inorg. Chem.* **1986**, *25*, 3010.
(19) Weterings, J. P.; Kent, T. A.; Prins, R. *Inorg. Chem.* **1987**, *26*, 324.
(20) Roth, E. K. H.; Greneche, J. M.; Jordanov, J. *J. Chem. Soc., Chem. Commun.* **1991**, 105.
(21) Coucouvanis, D.; Al-Ahmad, S.; Salifoglou, A.; Dunham, R. W.; Sands, R. H. *Angew. Chem., Int. Ed. Engl.* **1988**, *27*, 1353.
(22) Hagen, K. S.; Watson, A. D.; Holm, R. H. *J. Am. Chem. Soc.* **1983**, *105*, 3905–3913: $Fe_3S_4(SEt)_4]^{3-}$. (b) Hagen, K. S.; Holm, R. H. *J. Am. Chem. Soc.* **1982**, *104*, 5496: $(Fe_3S_4(SPh)_4]^{3-}$.
(23) Weigel, J. A.; Srivastava, K. K. P.; Day, E. P.; Munck, E.; Holm, R. H. *J. Am. Chem. Soc.* **1990**, *112*, 8015.
(24) Ciurli, S.; Yu, S.; Holm, R. H.; Srivastava, K. K. P.; Munck, E. *J. Am. Chem. Soc.* **1990**, *112*, 8169.
(25) Ross, B. L.; Grasselli, J. G.; Ritchey, W. M.; Kaesz, H. D. *Inorg. Chem.* **1963**, *2*, 1023.

added 0.33 g (1.18 mmol) of $Mo(CO)_3(CH_3CN)_3$ with stirring. After stirring for 20 min the resulting reaction mixture was filtered and to the filtrate were added 50 mL of THF and 100 mL of ether. Upon standing for 24 h a black crystalline solid formed. The solid was collected by filtration, washed with ether, and dried in vacuum: yield 0.8 g (60%). Anal. Calcd for $C_{48}H_{81}N_3O_3S_7Fe_3Mo$ (MW = 1236.23): C, 46.6; H, 6.62; N, 3.40. Found: C, 47.0; H, 6.70; N, 3.14.

Tris(tetraethylammonium) Tris(*p*-methoxythiophenolato)tris(μ_3-sulfido)triferrate(II,2III)-Molybdenum(0) Tricarbonyl, $(Et_4N)_3Fe_3S_4(SC_6H_4$-*p*-$OMe)_3Mo(CO)_3$ (III). To a solution of 1.0 g (1.08 mmol) of $(Et_4N)_3Fe_3S_4(SEt)_4$ in 30 mL of CH_3CN was added 0.61 g (4.3 mmol) of *p*-(methoxythio)phenol with stirring. After stirring for 20 min the color changed to purple. The solution was filtered, and the solvent was removed to dryness. The residue was washed several times with ether and then dissolved in 30 mL of CH_3CN. To the resulting solution was added 0.35 g (1.18 mmol) of $Mo(CO)_3(CH_3CN)_3$. After stirring for 20 min the reaction mixture was filtered and to the filtrate were added 50 mL of THF and 100 mL of ether. Upon standing for 24 h a black crystalline solid formed. The solid was collected by filtration, washed with ether, and dried in vacuum: yield 1.1 g (80%). Anal. Calcd for $C_{48}H_{81}N_3O_6S_7Fe_3Mo$ (MW = 1284.29): C, 44.9; H, 6.37; N, 3.27; S, 17.5; Fe, 13.0; Mo, 7.47. Found: C, 44.4; H, 6.13; N, 3.18; S, 16.99; Fe, 13.0; Mo, 6.70.

Tris(tetraethylammonium) Tris(phenoxy)tris(μ_3-sulfido)triferrate-(II,2III)-Molybdenum(0) Tricarbonyl, $(Et_4N)_3Fe_3S_4(OC_6H_5)_3Mo(CO)_3$ (IV). To a solution of 1.1 g (1.18 mmol) of $(Et_4N)_3Fe_3S_4(SEt)_4$ in 30 mL of CH_3CN was added 0.4 g (4.72 mmol) of phenol in 5 mL of CH_3CN with stirring. After stirring for 20 min the greenish-brown solution was filtered, and the solvent was removed under vacuum. The residue was washed several times with ether and then was dissolved in 30 mL of CH_3CN. To the resulting solution was added 0.33 g (1.18 mmol) of $Mo(CO)_3(CH_3CN)_3$, and after stirring for 30 min the reaction mixture was filtered and 150 mL of ether were added. Upon standing for 24 h a crystalline solid formed. The product was collected by filtration, washed with ether, and dried in vacuum: yield 0.8 g (65%). Anal. Calcd for $C_{45}H_{75}N_3O_6S_4Fe_3Mo$ (MW = 1145.96): C, 47.2; H, 6.61; N, 3.67; S, 11.9; Fe, 14.6; Mo, 8.37. Found: C, 47.3; H, 6.47; N, 3.54; S, 12.0; Fe, 14.7; Mo, 7.60.

Tris(tetraethylammonium) Tris(*p*-methoxythiophenolato)tris(μ_3-sulfido)triferrate(II,2III)-Tungsten(0) Tricarbonyl, $(Et_4N)_3[Fe_3S_4(p$-$OMeC_6H_4S)_3W(CO)_3]$ (V). To a solution of 1.0 g (1.08 mmol) of $(Et_4N)_3[Fe_3S_4(EtS)_4]$ in 30 mL of CH_3CN was added 0.61 g (4.3 mmol) of *p*-(methoxythio)phenol with stirring. After stirring for 20 min the color changed to purple. The solution was filtered, and the solvent removed to dryness. The residue was washed several times with ether and then dissolved in 30 mL of CH_3CN. To the resulting solution 0.43 g (1.1 mmol) of $W(CO)_3(CH_3CN)_3$ was added. After stirring for 20 min the reaction mixture was filtered and to the filtrate were added 50 mL of THF and 100 mL of ether. Upon standing for 24 h a black crystalline solid formed. The solid was collected by filtration, washed with ether, and dried in vacuum: yield 0.62 g (51%). Anal. Calcd for $C_{48}H_{81}N_3O_6S_7Fe_3W$ (MW = 1372.14): C, 42.0; H, 5.96; N, 3.06; Fe, 12.2; W, 13.4. Found: C, 41.7; H, 5.97; N, 2.87; Fe, 11.1; W, 14.2.

Tris(tetraethylammonium) Trichlorotris(μ_3-sulfido)triferrate-(II,2III)-Molybdenum(0) Tricarbonyl, $(Et_4N)_3[Fe_3S_4Cl_3Mo(CO)_3]$ (VI). To a stirred solution of 1.0 g (0.77 mmol) of $(Et_4N)_3[Fe_3S_4(p$-$OMeC_6H_4S)_3Mo(CO)_3]$ in 30 mL of CH_3CN was added a solution of C_6H_5COCl (0.32 g, 2.3 mmol) in 10 mL of CH_3CN over 30 min. The color gradually changed to purple. The reaction mixture was then filtered off, and ether was added to the filtrate. Upon standing for 10 h a black microcrystalline solid formed. The product was collected by filtration, washed with ether, and dried in vacuum: yield 0.7 g (75%). Anal. Calcd for $C_{27}H_{60}N_3O_3Cl_3S_4Fe_3Mo$ (MW = 973.19): C, 33.3; H, 6.23; N, 4.32; Fe, 17.2; Mo, 6.23. Found: C, 34.1; H, 6.5; N, 4.41; Fe, 16.6; Mo, 5.8.

$(Et_4N)_2Fe_3S_4Cl_3Mo(Cl_4$-cat$)(CH_3CN)$. (a) From $(Et_4N)_3Fe_3S_4Cl_3Mo(CO)_3$. A solution of 1.0 g (1.03 mmol) of $(Et_4N)_3Fe_3S_4Cl_3Mo(CO)_3$ in 30 mL of CH_3CN was treated with a CH_3CN solution of 0.25 g (1.03 mmol) of tetrachloro-1,2-benzoquinone over a period of 1 h. After stirring for 12 h at room temperature, the solvent was removed to dryness, and the residue was washed several times with acetone. The acetone washings were combined, and 100 mL of ether was added. Upon standing for several hours an oily residue formed. This residue was dissolved in 30 mL of CH_3CN, and 100 mL of ether was added. Upon standing overnight, a black solid formed. The product was collected by filtration, washed with ether, and dried in vacuum: yield 0.58 g (54%). The UV–vis spectrum in CH_3CN solution (490, 298 nm) and the near and far-IR spectra of the product are identical to those reported for $(Et_4N)_2Fe_3S_4Cl_3Mo(Cl_4$-cat$)(MeCN)$.[26]

(26) Palermo, R. E.; Holm, R. H. *J. Am. Chem. Soc.* **1983**, *105*, 4310.

(b) From $(Et_4N)_3Fe_6S_6Cl_6\{Mo(CO)_3\}_2$. To a solution of 1.2 g (0.8 mmol) of $(Et_4N)_3Fe_6S_6Cl_6\{Mo(CO)_3\}_2$ in 30 mL of CH_3CN was added a solution of 0.39 g (1.6 mmol) of tetrachloro-1,2-benzoquinone in 5 mL of CH_3CN dropwise over 1 h. After stirring for 12 h the solvent was removed to dryness, and the residue was washed with ether. The solid was then washed with acetone several times. The acetone washings were combined and treated with 100 mL of ether. Upon standing for several hours an oily residue formed. The residue was then twice recrystallized from a CH_3CN/ether mixture. The second recrystallization affords 0.6 g of black crystalline solid. The UV/vis in acetonitrile solution (490, 298 nm) and the near and far-IR spectra of the product are identical to those reported for $(Et_4N)_2Fe_3S_4Cl_3Mo(Cl_4$-cat$)(MeCN)$.[26]

$(Et_4N)_4Fe_6S_8(EtS)_6Mo_2(Cl_4$-cat$)_2$. To a solution of 1.0 g (0.9 mmol) of $(Et_4N)_3Fe_3S_4(EtS)_3Mo(CO)_3$ in 20 mL of acetonitrile was added 0.23 g (0.9 mmol) of tetrachloro-1,2-benzoquinone, and the solution was stirred for 24 h. The microcrystalline solid that formed was collected by filtration and washed with a 1:2 mixture of acetonitrile/ether to give 0.50 g (50%) yield of product. The absorption spectrum of the product in acetonitrile (390 nm) and the ^1H NMR spectrum in DMSO-d_6 53 (CH_2) and 4.25 (CH_3) ppm confirmed the identity of the product as $(Et_4N)_4Fe_6S_8(EtS)_6Mo_2(Cl_4$-cat$)_2$.[27]

$(Et_4N)_3Fe_6S_8(EtS)_9Mo_2$. To a solution of 1.0 g (0.9 mmol) of $(Et_4N)_3Fe_3S_4(EtS)_3Mo(CO)_3$ in 20 mL of CH_3CN was added 0.24 g (2 mmol) of EtSSEt, and the solution was stirred for 48 h. After that period of time, the solution was diluted with ether and left to stand for several hours. A solid formed which was collected by filtration and washed with ether. The product was recrystallized from CH_3CN/ether. The final recrystallization afforded an amount of 0.31 g (40% yield) of microcrystalline solid. The absorption spectrum in CH_3CN solution (390 nm) and the ^1H NMR spectrum in CD_3CN (52 (CH_2), 17.45 ppm (CH_3)) confirmed the identity of the product as $(Et_4N)_3Fe_6S_8(EtS)_9Mo_2$.[28]

$(Et_4N)_4Fe_6S_6Cl_6\{Mo(CO)_3\}_2$. An amount of 0.39 g (0.03 mmol) of $(Et_4N)_3Fe_3S_4Cl_3Mo(CO)_3$ was heated in 20 mL of acetonitrile at 50 °C for 25 min. The color of the solution changed, and a black solid formed. The reaction mixture was filtered, and ether was added to the filtrate. The crude product was obtained by filtration and washed with ether. The product was then recrystallized from a CH_3CN/ether mixture. A microcrystalline solid formed. The product was collected by filtration, washed with ether, and dried. The product was found to be identical to $(Et_4N)_4Fe_6S_6Cl_6\{Mo(CO)_3\}_2$.[29] The yield was 0.1 g (40%).

$(Et_4N)_4Fe_6S_6(OC_6H_4$-*p*-$COMe)_6\{Mo(CO)_3\}_2$. (a) From $(Et_4N)_3Fe_3S_4(OC_6H_4$-*p*-$COMe)_4$. A solution of 0.70 g (0.075 mmol) of $(Et_4N)_3Fe_3S_4(SEt)_3$ was stirred with 0.41 g (0.30 mmol) of *p*-$COMeC_6H_4OH$ for 15 min. The resulting reaction mixture was filtered, and the volatile materials were removed under vacuum. The residue was washed with ether and then acetonitrile. The acetonitrile washings were combined and stirred with 0.24 g (0.08 mmol) of $Mo(CO)_3(CH_3CN)_3$ for 1 h. The reaction mixture was filtered, and ether was added. Upon standing for several hours, a black crystalline solid and oil were obtained. The crystalline solid was separated and washed with ether. The UV/vis spectrum in CH_3CN (426 nm), the infrared spectrum (1897, 1832 cm^{-1}), and the proton NMR spectrum in CD_3CN confirmed the identity of the product as $(Et_4N)_4Fe_6S_6(OC_6H_4$-*p*-$COCH_3)_6\{Mo(CO)_3\}_2$.[29b] The oily product was recrystallized from a CH_3CN/ether mixture, and more product was obtained. The overall yield was 0.32 g (39%).

(b) From $(Et_4N)_3Fe_3S_4(SEt)_3Mo(CO)_3$·$CH_3CN$. A solution of 0.5 g (0.46 mmol) of $(Et_4N)_3Fe_3S_4(SEt)_3Mo(CO)_3$·$CH_3CN$ in 30 mL of CH_3CN was treated with 0.19 g (1.4 mmol) of HOC_6H_4-*p*-$COCH_3$ in 5 mL of CH_3CN over a period of 30 min. After stirring for another 30 min, the solution was filtered, and the filtrate was treated with diethyl ether. Upon standing overnight, a microcrystalline solid formed. The solid was collected, washed with ether, and dried in vacuum. An amount of 0.41 g (40% yield) of microcrystalline solid obtained. The UV/vis spectrum in acetonitrile (426 nm), the infrared spectrum (1897, 1832 cm^{-1}), and the proton NMR spectrum in CD_3CN solution confirmed the identity of the product as $(Et_4N)_4Fe_6S_6(OC_6H_4$-*p*-$COCH_3)_6\{Mo(CO)_3\}_2$.[29b]

X-ray Diffraction Measurements. Data Collection and Reduction. A single crystal of $[(C_2H_5)_4N]_3[Fe_3S_4(SC_2H_5)_3Mo(CO)_3$·$CH_3CN]$ was

(27) Wolff, T. E.; Power, P. P.; Frankel, R. B.; Holm, R. H. *J. Am. Chem. Soc.* **1980**, *102*, 4694.

(28) (a) Christou, G.; Garner, C. D. *J. Chem. Soc., Dalton Trans.* **1980**, 2363. (b) Christou, G.; Garner, C. D. *J. Chem. Soc., Dalton Trans.* **1980**, 2354. (c) Walff, T. E.; Berg, J. M.; Hodgson, K. O.; Holm, R. H. *J. Am. Chem. Soc.* **1979**, *101*, 4140. (d) Armstrong, W. H.; Mascharak, P. K.; Holm, R. H. *J. Am. Chem. Soc.* **1982**, *104*, 4373.

(29) (a) Salifoglou, A.; Kanatzidis, M. G.; Dunham, W. R.; Kostikas, A.; Simopoulos, A.; Coucouvanis, D. *Inorg. Chem.* **1988**, *27*, 4066. (b) Al-Ahmad, S. A.; Salifoglou, A.; Kanatzidis, M. G.; Dunham, W. R.; Coucouvanis, D. *Inorg. Chem.* **1990**, *29*, 927–938.

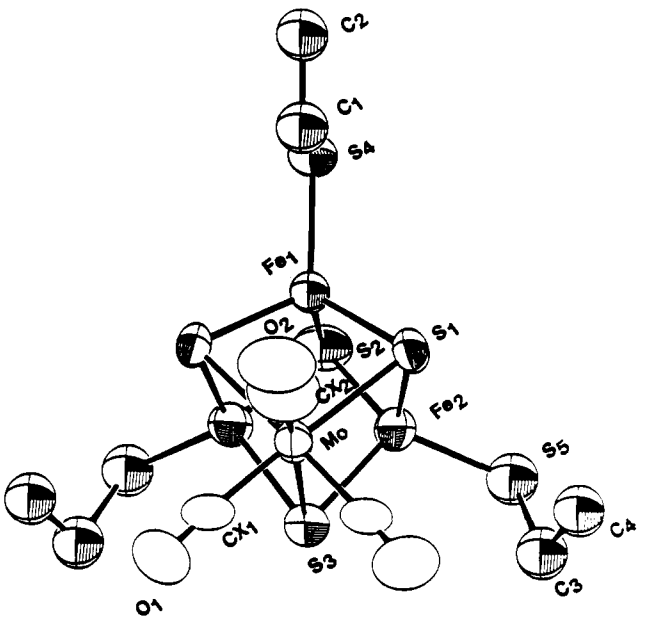

Figure 1. Structure and labeling of the anion in $(Et_4N)_3[Fe_3S_4(EtS)_3Mo(CO)_3]$ (**I**). Thermal ellipsoids as drawn by ORTEP represent the 40% probability surfaces. The thermal ellipsoids for the S_5 and C atoms of the EtS^- terminal ligands have been drawn smaller for clarity.

obtained by slow diffusion of a THF/ether mixture into an acetonitrile solution of the complex. The crystal was mounted in a thin walled capillary tube under nitrogen and then sealed to prevent exposure to air and moisture.

Diffraction data on $[(C_2H_5)_4N]_3[Fe_3S_4(S\text{-}C_2H_5)_3Mo(CO)_3\cdot CH_3CN]$ were collected with a Nicolet P3/F four circle computer controlled diffractometer, equipped with a molybdenum X-ray tube and a graphite monochromator. Crystal data and data collection parameters are summarized in ref 30. The final orientation matrix and unit cell parameters were determined from 15 machine-centered reflections. Two standard reflections, examined after every 100 measurements, showed no sign of decay during the course of data collection. Data reduction was carried out with the program XTAPE of the SHELXTL structure determination package. The systematic absences are consistent with the orthorhombic space group, *Pbcm*.

Solution and Refinement of the Structure. The direct method routine SOLV of the SHELXTL84 package of the crystallographic program was used to solve the structure. Trial positions for the molybdenum and iron atoms were taken from the E-map derived from the phase set with the highest combined figure of merit. The remaining non-hydrogen atoms were determined by difference Fourier maps. All non-hydrogen atoms were refined with anisotropic thermal parameters according to a protocol described previously.[29b]

The asymmetric unit cell consists of half of the anion, three half-cations, and a molecule of acetonitrile. The remaining atoms are generated by symmetry. Crystal structure parameters and final *R* values are given in ref 30. Positional parameters and selected interatomic distances have been deposited. The marginal quality of the first data set prompted us to obtain an additional data set from a different crystal and redetermine the structure.[30] The results of the second determination were nearly indistinguishable from those of the first determination, and the two have been compared in a previous communication.[21]

Crystallographic Results. The fractional atomic coordinates and equivalent isotropic thermal parameters, with standard deviations, for the non-hydrogen atoms in $(Et_4N)_3[Fe_3S_4(EtS)_3Mo(CO)_3\cdot CH_3CN]$ have been deposited together with the observed and calculated structure factors. The latter for the first data set have been deposited previously with ref 21. The structure of the anion is shown in Figure 1.

Synthesis

The fusion or reorganization reactions of the $[Fe_2S_2L_4]^{2-}$ and $[Fe_4S_4L_4]^{2-}$ clusters, induced by the $Mo(CO)_3(CH_3CN)_3$ reagent, lead to the formation of the octanuclear $[Fe_6S_6L_6\{Mo(CO)_3\}_2]^{3-,4-}$ clusters. These reactions not only demonstrate the remarkable stability of the octanuclear clusters but also suggest that the $Mo(CO)_3$ unit may serve as a "template" that brings together and facilitates the coupling of three solvated $[Fe_2S_2L_4]^-$ units.[29]

This apparent synthetic utility prompted us to explore the effectiveness of the $M(CO)_3$ units in the template coupling of other Fe/S clusters. The $[M(CO)_3Fe_3S_4L_3]^{3-}$, M = Mo, W, clusters were obtained as a result of the $M(CO)_3$ promoted rearrangement of the known,[22a] linear, $(Et_4N)_3[Fe_3S_4(EtS)_4]$ cluster (eq 2).

$$[Fe_3S_4L_4]^{3-} + Mo(CO)_3(CH_3CN)_3 \rightarrow [Mo(CO)_3Fe_3S_4L_3]^{3-} \quad (2)$$

The yields of $[Fe_3S_4(EtS)_3Mo(CO)_3]^{3-}$, **I**, $[Fe_3S_4(BzS)_3Mo(CO)_3]^{3-}$, **II**, $[Fe_3S_4(p\text{-}OMePhS)_3Mo(CO)_3]^{3-}$, **III**, $[Fe_3S_4(PhO)_3Mo(CO)_3]^{3-}$, **IV**, and $[Fe_3S_4(p\text{-}MeOC_6H_4S)_3W(CO)_3]^{3-}$, **V**, can be optimized by adjusting the reaction conditions. These clusters are readily isolated from acetonitrile solutions in the form of tetraethylammonium salts. The indicated cubane structure has been demonstrated by X-ray diffraction for the SEt derivative. The analogous tungsten cluster can also be prepared using $W(CO)_3(CH_3CN)_3$.

The reaction systems investigated to make several derivatives of $[M(CO)_3Fe_3S_4L_3]^{3-}$, involve substitution of the ethanethiolate ligand in the $[Fe_3S_4(EtS)_4]^{3-}$ cluster under conditions sufficiently mild to avoid significant decomposition of the $[Fe_3S_4]$ core. This objective can be achieved by the reaction of the free thiols or phenol with the $[Fe_3S_4(EtS)_4]^{3-}$ complex and generation of the volatile and easily removed EtSH. When C_6H_5OH and HSC_6H_5-*p*-OMe were reacted with $[Fe_3S_4(EtS)_4]^{3-}$, the amount of the acid form of the added ligand was stoichiometric and the reaction proceeded to full substitution in 10–15 min. The use of the less acidic benzylthiol ($HSCH_2C_6H_5$), in the same reaction, does not proceed as fast as when using aromatic thiol or phenol, and an excess thiol is required to shift the equilibrium in favor of the desired product. The corresponding substituted trimers can be obtained in an excellent yield and high purity without any decomposition. The success of these reactions (vide infra) depend upon the prior knowledge of the relative tendencies of the added thiols or phenol to replace the coordinated ethanethiolate ligand. These facile substitution reactions also have been observed and reported for the $[Fe_4S_4(t\text{-}BuS)_4]^{2-}$ cubane cluster.[31]

The $(Et_4N)_3[Fe_3S_4Cl_3Mo(CO)_3]$, **VI**, cluster is made by substituting the thiol ligand with chloride ions using benzoyl chloride in acetonitrile. This route has been used successfully in the preparation of Fe/Mo/S and Fe/S clusters which have halides as terminal ligands.[26,31b] This cluster is not very stable in solutions and transforms in acetonitrile solutions to the corresponding prismane 2/1 adduct $(Et_4N)_4[Fe_6S_6Cl_6\{Mo(CO)_3\}_2]$.

Stability of the $[MoFe_3S_4]^0$ Core. In the course of synthesizing the $[MoFe_3S_4L_3]^{3-}$ clusters from the linear trinuclear precursors, several observations were noticed. (a) Attempts to synthesize the single cubane with SPh or SPh-*p*-Me as terminal ligands failed. The only stable and characterizable single cubane cluster with thiophenol is obtained when SC_6H_4-*p*-OMe is used as a terminal ligand. (b) The most stable tungsten clusters obtained are those with SC_6H_4-*p*-OMe and EtS as terminal ligands on the iron sites.

Solutions of $[MoFe_3S_4L_3]^{3-}$ clusters in deuterated acetonitrile exhibit clean isotropically shifted spectra. However, upon standing overnight, new peaks were observed. These new peaks were

(30) Summary of crystal data, intensity collection, and structure refinement of $(Et_4N)_3Fe_3S_4(SC_2H_5)_3Mo(CO)_3\cdot CH_3CN$, I: The values in brackets represent values and results of a structure determination on a second data set obtained from an independently grown new crystal: crystal size (mm), 0.15 × 0.58 × 0.75 (0.20 × 0.40 × 0.60); unit cell dimensions, a = 16.557 (5) Å [16.563 (4) Å], b = 18.915 (6) Å [18.879 (6) Å], c = 17.110 (6) Å [17.108 (5) Å]. $\alpha = \beta = \gamma = 90°$; space group *Pbcm*, Z = 4, d_{calcd} = 1.35 g cm^{-3}, d_{obsd} = 1.40 g cm^{-3}, μ = 12.9 cm^{-1}; $2\theta_{max}$ = 40 (Mo, λKα, 0.71069 Å); unique reflections, 2620, used in refinement, $F_o^2 > 3\sigma(F_o^2)$, 1290 [1376]; parameters 198, final R = 6.99% [7.33%], R_w = 6.47% [6.89%]. The low number of observed reflections, for both data sets, is due to our inability to obtain crystals of high crystallographic quality. This problem, coupled with positional disorders encountered with two of the three Et_4N^+ cations, accounts for the rather high temperature factors obtained for some of the carbon atoms.

(31) (a) Averill, B. A.; Herskovitz, T.; DePamphilis, B. V.; Que, L., Jr.; Holm, R. H. *J. Chem. Soc.* **1974**, *96*, 4159. (b) Johnson, R. W.; Holm, R. H. *J. Am. Chem. Soc.* **1978**, *100*, 5338.

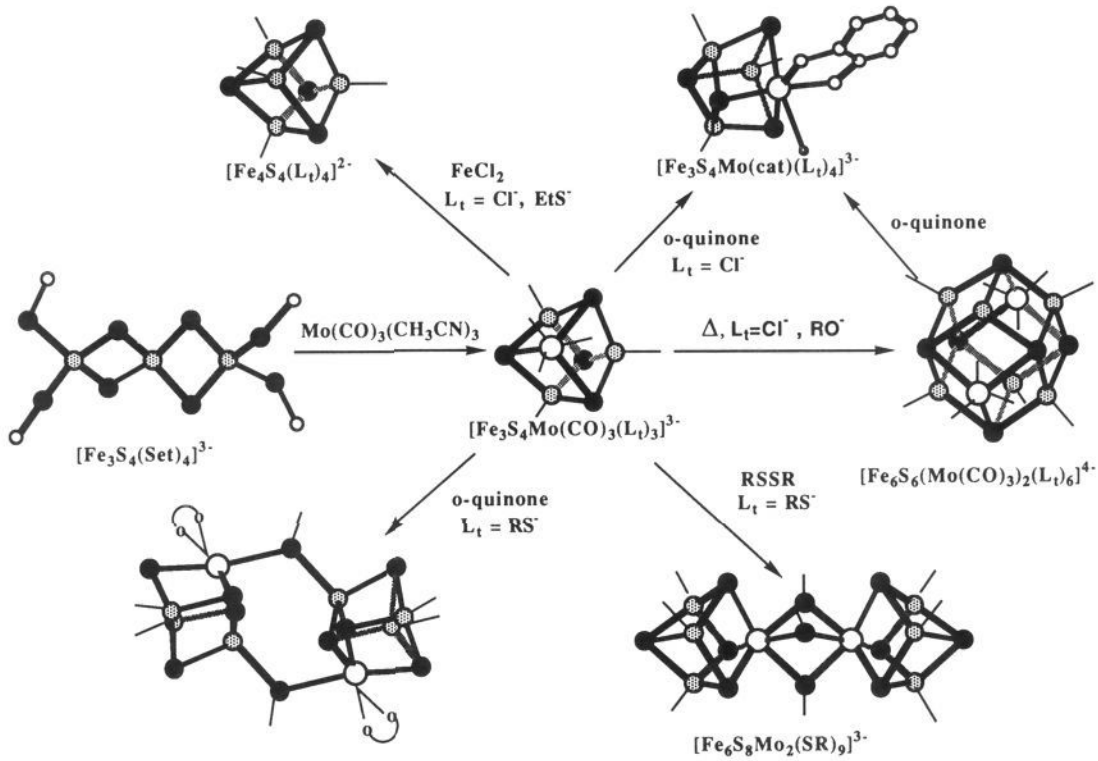

Figure 2. The synthetic versatility of the $[Fe_3S_4(L)_3Mo(CO)_3]^{3-}$ clusters.

assigned to the $[Fe_6S_9(SEt)_2]^{4-}$ and $[Fe_4S_4(SEt)_4]^{2-}$ clusters[22a] and $[Fe_4S_4L_4]^{2-}$ for L = SPh-*p*-OMe, OPh, and SBz.[31] These species are formed as a result of the disproportionation of the $MoFe_3S_4$ core in solution.

Reactions of the phenoxy linear trimer $[Fe_3S_4(OC_6H_4\text{-}p\text{-}COMe)_4]^{3-}$ with $Mo(CO)_3(MeCN)_3$ under the same conditions employed to prepare other single cubanes $[Mo(CO)_3Fe_3S_4L_3]^{3-}$ clusters do not afford the desired product. Instead, a moderate yield of the octanuclear cluster $[Fe_6S_6(OC_6H_4\text{-}p\text{-}COMe)_6\{Mo(CO)_3\}_2]^{4-}$ was obtained as the ultimate product.[29b] It is clear that the single cubane core with OC_6H_4-*p*-COMe as a terminal ligand at the iron site is not stable in the cubane form. It is believed that the single cubane $[Mo(CO)_3Fe_3S_4(OC_6H_4\text{-}p\text{-}COMe)_3]^{3-}$ forms first, and, due to its thermodynamic instability, it transforms to the octanuclear cluster. This transformation occurs at room temperature in acetonitrile solution.

When a solution of $[Mo(CO)_3Fe_3S_4(SEt)_3]^{3-}$ is reacted with 3 equiv of HOC_6H_4-*p*-COMe in acetonitrile, the only product obtained is $[Fe_6S_6(OC_6H_4\text{-}p\text{-}COMe)_6\{Mo(CO)_3\}_2]^{4-}$[29b] in moderate yield.

Reactions of the $[MoFe_3S_4L_3]^{3-}$ Clusters. The reactions of the $[Fe_3S_4L_3Mo(CO)_3]^{3-}$ clusters and the diversity in their synthetic utility are summarized in Figure 2. The reaction of $[Fe_3S_4Cl_3Mo(CO)_3]^{3-}$ with 1 equiv of tetrachloro-1,2-benzoquinone in acetonitrile over 12 h resulted in the complete decarbonylation of the molybdenum atom and the coordination of the catecholate ligand to the molybdenum site. This reaction takes place without core rearrangement. It is expected that the first step in this reaction is the oxidation of the $Mo(CO)_3$ unit by two electrons which would result in the formation of the intermediate $[Mo^{II}(CO)(cat)]$ subunit. However, the expected intermediate in this reaction, $[Fe_3S_4Cl_3Mo^{II}(cat)(CO)]^{3-}$, was not isolated from the reaction mixture. The assumption is that the intermediate species forms in solution and then undergoes internal oxidation that results in the complete decarbonylation of the molybdenum site in $[Fe_3S_4Cl_3Mo^{II}(cat)(CO)]^{3-}$ and formation of the solvated and previously reported single cubane $[Fe_3S_4Cl_3Mo(cat)(CH_3CN)]^{2-}$.[26] The latter also is obtained readily by the oxidative decarbonylation of the $[Fe_6S_6Cl_6\{Mo(CO)_3\}_2]^{3-}$ prismane adduct[32] with 2 equiv of Cl_4-1,2-benzoquinone. In this reaction, core rearrangement is observed. Presumably, the reorganization step(s) take place after the oxidation has taken place at the molybdenum site and not decomposition of the prismane adduct to single-cubane, followed by oxidation of the molybdenum atoms. This suggestion relies on the conclusion extracted from the reactions of $[Fe_6S_6Cl_6\{Mo(CO)_3\}_2]^{3-,4-}$ with sulfide ions or sulfur. Neither of these reactions afford the corresponding single cubane cluster.

To investigate the effect of the terminal ligand on the iron site on the pathway of the oxidation reaction with quinone, the $[Fe_3S_4(SEt)_3Mo(CO)_3]^{3-}$ cluster was oxidized with tetrachloro-1,2-benzoquinone under the same conditions as above. In this case, the products isolated from this reaction mixture do not show carbonyl absorption in the infrared spectra. The spectroscopic properties of the purified product are identical to those reported for the doubly-bridged, double-cubane clusters with the formula $[Fe_6S_8(SEt)_6Mo_2(cat)_2]^{4-}$.[27] For this reaction, we also suggest that the oxidation takes place preferentially at the molybdenum site. The doubly-bridged, double-cubane forms, rather than the solvated single cubane, presumably due to the superior ability of the thiolate ligands to serve as bridging ligands. The doubly-bridged, double-cubane cluster is known to undergo dissociation in coordinating solvents such as DMSO and CH_3CN and forms the solvated single cubanes.

The $[Mo(CO)_3Fe_3S_4(SEt)_3]^{3-}$ clusters reacted with EtSSEt in acetonitrile solution, and the product was found to be identical to the double-cubane cluster $[Mo_2Fe_6S_8(SEt)_6(\mu_2\text{-}SEt)_3]^{3-}$ reported previously.[28]

The reaction of $[Mo(CO)_3Fe_3S_4(SEt)_3]^{3-}$ with anhydrous $FeCl_2$ in acetonitrile resulted in complete substitution of the $Mo(CO)_3$ fragment with an FeCl fragment. This reaction was monitored by ^1H NMR spectroscopy; within 20 min, the resonances assigned

(32) (a) Coucouvanis, D.; Kanatzidis, M. G. *J. Am. Chem. Soc.* **1985**, *107*, 5005. (b) Kanatzidis, M. G.; Coucouvanis, D. *J. Am. Chem. Soc.* **1986**, *108*, 337. (c) Salifoglou, A.; Kanatzidis, M. G.; Coucouvanis, D. *J. Chem. Soc., Chem. Commun.* **1986**, 559. (d) Coucouvanis, D.; Salifoglou, A.; Kanatzidis, M. G.; Simopoulos, A.; Kostikas, A. *J. Am. Chem. Soc.* **1987**, *109*, 3807. (e) Coucouvanis, D.; Salifoglou, A.; Kanatzidis, M. G.; Dunham, W. R.; Simopoulos, A.; Kostikas, A. *Inorg. Chem.* **1988**, *27*, 4066–4077.

Table I. Selected Intracube Distances and Angles for the Heteronuclear $[MFe_3S_4(L)_4]^{n-}$ Cubanes in $[Et_4N]_3[Mo(CO)_3Fe_3S_4(SEt)_3]$ (I), $[Et_4N]_3[MoFe_3S_4(SEt)_3(Cl_4cat)(CN)]$ (A), $[Me_4N][VFe_3S_4(Cl)_3(DMF)_3]\cdot 2DMF$ (B), and $[Et_4N]_3[NiFe_3S_4(SEt)_3(PPh_3)]$ (C)

	I	A[a]	B[b]	C[c]
		Distances[d]		
M[e]–Fe	3.248 (4, 17)	2.741 (3, 11)	2.777 (3, 5)	2.69 (2)
range	3.225 (4)–3.274 (5)			
Fe–Fe	2.735 (4, 6)	2.708 (3, 11)	2.707 (3, 27)	
range	2.723 (6)–2.742 (4)			
M[e]–S_b	2.631 (4, 10)	2.376 (3, 12)	2.336 (3, 5)	2.262 (6)
range	2.611 (8)–2.651 (6)			
Fe–S_b	2.263 (6, 8)	2.272 (6, 8)	2.271 (6, 3)	2.269 (7), 2.306 (8)
range	2.246 (8)–2.280 (6)			
Fe–S_d[f]	2.298 (4, 10)	2.280 (3, 9)	2.292 (3, 5)	2.297 (8)
range	2.289 (9)–2.304 (8)			
Fe–S_t(Cl)	2.293 (4, 10)	2.262 (3, 10)	2.266 (3, 8)	2.283 (6)
range	2.283 (6)–2.301 (8)			
		Angles		
Fe–M–Fe	49.92 (4, 8)	59.2 (3, 4)	58.3 (3, 4)	
range	49.81 (5)–50.13 (5)			
Fe–Fe–M	65.10 (4, 7)	60.5 (4, 2)	60.7 (4, 1)	
range	64.00 (7)–66.26 (6)			
Fe–Fe–Fe	59.9 (4, 1)	59.5	59.4	
range	59.7 (1)–60.2 (1)			
S_b–M–S_b	87.2 (4, 5)	102.5 (3, 15)	102.0 (3, 5)	105.8 (7)
range	86.4 (2)–88.0 (2)			
Fe–S_d–Fe[f]	72.9 (4, 5)	72.9 (3,5)		
range	72.2 (5)–73.4 (2)			
Fe–S_b–Fe	74.2 (4, 1)	73.2 (6, 6)	72.8 (6, 9)	
range	74.1 (1)–74.3 (1)			

[a] From ref 34. [b] From ref 14b. [c] From ref 24. The distances and angles are reported under idealized C_3 symmetry. [d] Mean values of crystallographically independent, chemically equivalent, structural parameters. The first number in parentheses represents the number of chemically equivalent bond lengths and angles averaged out; the second number represents the larger of the individual standard deviations or the standard deviation from the mean, σ. $\sigma = [\sum_{i=1}^{N}(x_i - \bar{x})^2/N(N-1)]^{1/2}$. [e] M = Mo for I and A and V and Ni for B and C, respectively. [f] S_d is the μ_3 sulfide diagonally across M.

for $[Mo(CO)_3Fe_3S_4(SEt)_3]^{3-}$ disappeared, and new resonances at 12.7, 13.5, and 14.4 ppm were observed. These resonances are assigned to the mixed-ligand $[Fe_4S_4(SEt)_{4-n}Cl_n]^{2-}$ species. The 12.7 ppm signal is assigned for the CH_2 group resonances of the $[Fe_4S_4(SEt)_4]^{2-}$ cluster, and the 13.5 and 14.4 signals are assigned to the $[Fe_4S_4(SEt)_3Cl]^{2-}$ and $[Fe_4S_4(SEt)_2Cl_2]^{2-}$ mixed-ligand cubanes, respectively. This assignment is based on the results obtained when a solution of $[Fe_4S_4(SEt)_4]^{2-}$ is treated with 1 and 2 equiv of PhCOCl.[22] The presence of the three mixed ligand species is due to the disproportionation of the $[Fe_4S_4(SEt)_3Cl]^{2-}$ cluster.

In this reaction, there was no evidence for the formation of $[Fe_6S_9(SEt)_2]^{4-}$ or $[Fe_3S_4(SEt)_4]^{3-}$. This reaction demonstrates the ability of the (FeCl) fragment to substitute $Mo(CO)_3$ and result in the formation of a more stable cubane.

The above reactions, and particularly the oxidative decarbonylation reactions, despite the moderate yields obtained, demonstrate the utility of the $[Fe_3S_4L_3Mo(CO)_3]^{3-}$ clusters, as interesting precursors for the synthesis of other Mo/Fe/S clusters that are obtained only by the "spontaneous self-assembly"[33] route.

Description of Structure. Selected interatomic distances and bond angles for the $[Fe_3S_4(SC_2H_5)_3Mo(CO)_3]^{3-}$ anion and synoptic data for the cations are collected in Table I. The most important structural features of the $[Fe_3S_4(SC_2H_5)_3Mo(CO)_3]^{3-}$ anion (Figure 1) are as follows: (1) The cluster has a crystallographically imposed mirror plane containing the atoms Mo, S_2, S_3, Fe_1, S_4, C_1, C_2, CX_2, and O_2 and the cluster contains two types of Fe sites, Fe_1 in the mirror plane and Fe_2, Fe_2' related by the plane. (2) Each Fe atom is found with an approximate tetrahedral geometry. (3) The Mo atom exhibits a distorted octahedral geometry. The coordination environment around the molybdenum atom consists of three carbon monoxide ligands and three μ^3-sulfides (S_1, S_1', and S_3). A close examination of the crystallographic results (Table I) reveals some rather unusual structural features. By comparison to the $[MoFe_3S_4]^{3+}$ cores in the clusters reported by Palermo et al.,[34] the $[MoFe_3S_4]^0$ core in I (Table I) shows a pronounced trigonal elongation along the $[MoFe_3S_4]$ body diagonal that contains S_4 and the Mo atom. This distortion is a consequence of weak $Mo(CO)_3$–Fe_3S_4 bonding interactions and is manifested by the unusually long Mo–S bonds and Mo–Fe distances in I. The Mo–S bonds at 2.631 Å and the Mo–Fe distances at 3.247 Å are longer than the weak Mo–S bonds and long Mo–Fe distances in the $Fe_6S_6(OC_6H_4\text{-}p\text{-}R)_6[Mo(CO)_3]_2]^{4-}$[29] cluster at 2.61 and 3.00 Å, respectively. The Mo–CO bond length in I at 1.91 Å is indicative of the zero valence oxidation state of the Mo atom. The distorted tetrahedral coordination at each iron site is completed by a terminal ethanethiolate ligand. The Fe–S and Fe–SEt bond lengths in I, at 2.26 and 2.292 (8) Å, respectively, are similar to those reported previously for clusters with the $[MoFe_3S_4]^{3+}$ cores. The structural data are consistent with the Moessbauer spectra (vide infra) that indicate an average oxidation level for the iron atoms of 2.66, not unlike the one reported for the $[MoFe_3S_4]^{3+}$ cores. It appears that the oxidation state difference between the $[MoFe_3S_4]^0$ core in I and the $[MoFe_3S_4]^{3+}$ cores in the $[MoFe_3S_4Cl_3Mo(catecholate)(L^{-n})]^{(2+n)-}$ clusters is tied to the Mo atom. The $[Fe_3S_4]^0$ cluster appears to be a versatile ligand that can coordinate to either Mo^0 stabilized by π acceptor ligands or to Mo(III) bound to π donor ligands.

Electrochemical Measurements. Cyclic voltammetric data for the clusters I–VI, obtained in methylene chloride solutions on a platinum electrode vs SCE and using $(n\text{-}Bu)_4NClO_4$ as a supporting electrolyte, are presented in Table II. All complexes exhibit two reversible waves. The first wave occurs between −30 and −400 mV, while the second occurs at a potential around 500 mV more negative than the first one. In addition, each of these clusters exhibit an irreversible multielectron oxidation wave at a positive potential. This oxidation is expected to be centered at the molybdenum site and probably results in the oxidative decarbonylation of the molybdenum atom.

The shape, ΔE, and i_{ca}/i_{pa} ratios indicate that these waves are reversible in the electrochemistry time scale. The first wave is

(33) Holm, R. H. *Chem. Soc. Rev.* **1981**, *10*, 455–490.

(34) Palermo, R. E.; Singh, R.; Bashkin, J. K.; Holm, R. H. *J. Am. Chem. Soc.* **1984**, *106*, 2600.

Table II. Infrared, ^1H NMR, Electronic Spectra, and Cyclic Voltammetric Data for $[Fe_3S_4(EtS)_3Mo(CO)_3]^{3-}$ (I), $[Fe_3S_4(BzS)_3Mo(CO)_3]^{3-}$ (II); $[Fe_3S_4(p\text{-}OMePhS)_3Mo(CO)_3]^{3-}$ (III), $[Fe_3S_4(PhO)_3Mo(CO)_3]^{3-}$ (IV), $(Et_4N)_3Fe_3S_4(p\text{-}OMePhS)_3W(CO)_3$ (V), and $(Et_4N)_3[Fe_3S_4Cl_3Mo(CO)_3]$ (VI)

compd	IR, ν-CO[a] (cm^{-1})	^1H NMR[b] (δ)	electr spectr[c] (nm, $\times 10^{-3}$)	CV,[d] E_p (V), ΔE (mV), i_a/i_c
I	1864, 1750	(CH_3), 5.85 ($FeSCH_2$), 66	390, 19.3	$2^-/3^-$, −0.36, 122, 0.96 $3^-/4^-$, −0.89, 108,
II	1868, 1752	*o*-H, −7.38 *m*-H, 7.9 *p*-H (R), 6.25	382, 20.2	$2^-/3^-$, −0.29, 140, 0.96 $3^-/4^-$, −0.83, 108,
III	1866, 1760	*o*-H, −5.52 *m*-H, 13.6 *p*-H, 4.35	430, 17.7	$2^-/3^-$, −0.24, 123, 0.96 $3^-/4^-$, −0.79, 150,
IV	1868, 1756	*o*-H, 9.5 *m*-H, 18.15 *p*-H, 22.0	400, 18.3	$2^-/3^-$, −0.21, 160, 0.85 $3^-/4^-$, −0.78, 170
V	1855, 1756	*o*-H, −6.11 *m*-H, 13.7	442, 18.1	$2^-/3^-$, −0.30, 130, 0.96 $3^-/4^-$, −0.88, 140
VI	1877, 1773		534, 14.9	$2^-/3^-$, −0.03, 120, 0.96

[a] Obtained in KBr discs. [b] In CD_3CN solution at ambient probe temperature. In addition to the resonances attributed to I the NMR spectrum shows a minor component (~15%) with resonances at 12.7 and 2.4 ppm that is due to the $[Fe_4S_4(SEt)_4]^{2-}$ cluster. The latter is indeed a decomposition product of I. [c] Obtained in CH_3CN solution. [d] Obtained on a Pt electrode in CH_2Cl_2 solution vs a SCE reference electrode. For all measurements the scan rate was 200 mV/s. Normally the Et_4N^+ salts of the clusters are not very soluble in CH_2Cl_2; however, in the presence of excess $n\text{-}Bu_4NClO_4$ as the supporting electrolyte they readily go into solution.

due to the $2^-/3^-$ redox couple (oxidation), while the second wave is assigned to the $3^-/4^-$ redox couple (reduction) (eq 3).

$$[MoFe_3S_4]^{1+} \rightarrow [MoFe_3S_4]^0 \rightarrow [MoFe_3S_4]^{1-} \quad (3)$$

The first peak potential of these clusters varies from −0.03 V, for the $[Mo(CO)_3Fe_3S_4(Cl)_3]^{3-}$ analogue, to −0.40 V for $[Mo(CO)_3Fe_3S_4(EtS)_3]^{3-}$. The two redox potentials for the $[MoFe_3S_4]^0$ core clusters show a striking resemblance to those of the $[Fe_6S_6L_6\{Mo(CO)_3\}_2]^{3-,4-}$ complexes.[29] Furthermore, the variation in the values of the potential for these clusters for L = *p*-OMePhS$^-$, PhO$^-$ and for L = EtS$^-$, BzS$^-$, PhO$^-$, *p*-OMePhS$^-$, and Cl$^-$ parallels the one observed in the reduction potentials of the $[Fe_6S_6L_6\{Mo(CO)_3\}_2]^{3-}$[29] $[Fe_6S_8(SR)_9Mo_2]^{3-}$[28] and $[Fe_4S_4(SR)_4]^{2-}$ clusters.[35] The tungsten analogue, $[Fe_3S_4(SC_6H_4\text{-}p\text{-}OMe)_3W(CO)_3]^{3-}$, shows the same pattern of electrochemistry. Substitution of the molybdenum by tungsten results in a shift of the two reduction waves by 60 and 90 mV toward more negative values. Qualitatively the same behavior has been observed previously for clusters that contain the $[MFe_3S_4]^{3+}$ cores.[27]

Proton NMR Spectroscopy. In acetonitrile solution all clusters that contain ligand protons exhibit isotropically shifted ^1H NMR spectra (Table II). The alternating signs of the isotropic shifts of the phenyl ring protons resonances is typical for Ar–X–M (X = S, O, Se) paramagnetic complexes. It has been attributed previously to a dominant Fermi delocalization mechanism.[36] In the $(Et_4N)_3[Mo(CO)_3Fe_3S_4(SPh\text{-}p\text{-}OMe)_3]$, the ortho signal is identified by its relative broadness due to relaxation effects induced by its proximity to the paramagnetic center. The *o*-H, *m*-H, and *p*-OCH_3 resonances are observed at −5.5, 13.6, and 4.35 ppm, respectively. The analogous $(Et_4N)_3[W(CO)_3Fe_3S_4(SPh\text{-}p\text{-}OMe)_3]$ cluster shows *o*-H, *m*-H, and *p*-OCH_3 resonances at −6.1, 13.7, and 4.58 ppm, respectively. The following features apply to the spectra of all clusters in deuterated acetonitrile. (i) The resonances of the ligands' protons in $[Mo(CO)_3Fe_3S_4(OPh)_3]^{3-}$ are observed at lower fields than those of the prismane adducts, $[Fe_6S_6(OC_6H_4\text{-}p\text{-}R)_6\{Mo(CO)_3\}_2]^{n-}$,[29] and at a higher field than those of the $[Mo(cat)(MeCN)Fe_3S_4(SPh)_3]^{2-}$[28d] cluster. (ii) Substituting molybdenum by tungsten in the $[MFe_3S_4]$ core clusters resulted in larger isotropic shifts and a narrow line width of the ^1H NMR signals. A similar effect on the isotropic shift of the proton resonances has already been observed in heterometallic clusters containing iron and molybdenum or tungsten.[28]

Infrared Spectroscopy. The $[Fe_3S_4L_3Mo(CO)_3]^{3-}$ clusters show a doublet in the IR spectra for the coordinated carbonyl ligands. These absorption bands are assigned to the asymmetric E and symmetric A vibrational modes of the $Mo(CO)_3$ fragment which exhibits a local C_{3v} symmetry. Each cluster obtained shows a strong clean doublet in the CO terminal region that is indicative of pure product (Table II). The changes in the CO absorption energies are consistent with the changes in the nature of the terminal ligand (relative electronegativity) on the iron site. With chloride ion as a terminal ligand, the CO absorptions are observed at 1877 and 1773 cm^{-1}; with EtS as terminal ligand, the CO absorptions are observed at 1868 and 1750 cm^{-1}. Similar changes, affected by the nature of the terminal ligand, have been observed in the $[Fe_6S_6L_6\{Mo(CO)_3\}_2]^{3-,4-}$ (L = Cl, Br, I, and OC_6H_4-*p*-R) clusters.[29] The CO stretching vibration frequencies in the $[Fe_3S_4L_3Mo(CO)_3]^{3-}$ clusters are observed at a lower values compared to the vibrational frequencies of $Mo(CO)_3$ moiety in similar environments.[37] The low energy vibrations of the carbonyl ligands indicate that the Fe_3S_4 core is a poor π acceptor ligand. By comparison, the higher CO vibrational frequencies in the $[Fe_6S_6L_6\{Mo(CO)_3\}_2]^{3-,4-}$ clusters[29] indicate that the $[Fe_6S_6]^{3+}$ core is a better π acceptor "ligand" than the $[Fe_3S_4]^0$ core. This observation is also noticeable from the structure's metric data that show slightly longer Mo–S and short Mo–CO bond lengths in the $[Fe_3S_4(SEt)_3Mo(CO)_3]^{3-}$ cluster.

Electronic Spectra. The absorption spectra of the molybdenum and tungsten clusters, **I–VI**, in acetonitrile solutions (Table II) are dominated by an intense absorption band in the visible region. Another absorption in the UV region is also observed. These absorptions are useful for characterization purposes but are not sufficient to establish the purity of these clusters. The spectra of the $[MFe_3S_4]^0$ core clusters resemble those of the $[Mo_2Fe_6S_8(RS)_9]^{3-}$ and $[Mo_2Fe_6S_8(RS)_6(cat)_2]^{4-}$ clusters in aprotic solvents in that they contain two principle absorption bands.[28] The two bands presumably arise from ligand to core charge transfer excitation. The small bathochromic shift of the band maxima observed in the tungsten vs molybdenum $[MFe_3S_4]^0$ clusters has been observed previously in other $[MFe_3S_4]^{3+}$ cubane clusters.[27]

Moessbauer Spectroscopy. Moessbauer spectra were obtained at 125 K for the complexes **I–VI**. The general aspect of the line profiles was an asymmetric doublet with a high velocity line indicating, at various degrees of definition, the presence of more than one iron site. In view of the low definition available at this temperature the values of δ and Δ_{Eq} for the individual component doublets apparent in the spectral profiles cannot be determined very accurately. This was done more reliably at 4.2 K where the resolution is enhanced as shown below for complexes I and **II**. The *average* values however reported in Table III are well defined and can be used to characterize the average valence state of the Fe atoms in these complexes. For an FeS_4 tetrahedral unit, the isomer shift (IS) values for Fe(III) and Fe(II) are 0.25 and 0.7 mm/s, respectively, and a change in the isomer shift that accompanies an Fe valence change of 1 is ca. 0.45 mm/s. Furthermore, for a cluster with [***n***] electronically equivalent iron sites, a change in the oxidation level by [**1**] unit would roughly correspond to a change in the isomer shift value of $[1/n(0.45)]$.[32e] Under these empirical rules, the average isomer shift value of 0.43 mm/s for I would indicate that the Fe atoms in I are in a +2.67 formal oxidation state implying two Fe^{3+} and one Fe^{2+} ions. The similarity in the Fe formal oxidation levels in the $[MoFe_3S_4]^0$ core of I and in the previously reported[38,39] $[MoFe_3S_4]^{3+}$ cores suggests that, while the latter formally contain Mo(III), the former contains

(35) Laskowski, E. J.; Frankel, R. B.; Gillum, W. O.; Papaefthymiou, G. C.; Renaud, J.; Ibers, J. A.; Holm, R. H. *J. Am. Chem. Soc.* **1978**, *100*, 5322.
(36) (a) Holm, R. H.; Phillips, W. D.; Averill, B. A.; Mayerle, J. J.; Herskovitz, T. *J. Am. Chem. Soc.* **1974**, *96*, 2109. (b) Reynolds, J. G.; Laskowski, E. J.; Holm, R. H. *J. Am. Chem. Soc.* **1978**, *100*, 5315.
(37) (a) Ashby, M. T.; Lichtenberg, D. L. *Inorg. Chem.* **1985**, *24*, 636. (b) Backes Dahmann, G.; Wieghhardt, K. *Inorg. Chem.* **1985**, *24*, 4049. (c) Cotton, F. A.; Zingales, F. *Inorg. Chem.* **1962**, *1*, 145. (d) Abel, E. W.; Bennett, M. A.; Wilkinson, G. *J. Chem. Soc. Part III* **1959**, 2323.
(38) Carny, M. J.; Kovacs, J. A.; Zhang, Y. P.; Papaefthymiou, G. C.; Spartalian, K.; Frankel, R. B.; Holm, R. H. *Inorg. Chem.* **1987**, *26*, 719.

Table III. ^{57}Fe Moessbauer Parameters[a] Obtained at 125 K in Zero Applied Field vs Fe for $[Fe_3S_4(SEt)_3Mo(CO)_3]^{3-}$ (I), $[Fe_3S_4(SBz)_3Mo(CO)_3]^{3-}$ (II), $[Fe_3S_4(SPh\text{-}p\text{-}OMe)_3Mo(CO)_3]^{3-}$ (III), $[Fe_3S_4(OPh)_3Mo(CO)_3]^{3-}$ (IV), $(Et_4N)_3Fe_3S_4(SPh\text{-}p\text{-}OMe)_3W(CO)_3$ (V), and $(Et_4N)_3[Fe_3S_4Cl_4o(CO)_3]$ (VI)

compd	δ_1 (mm/s)	Δ_{Eq1} (mm/s)	δ_2 (mm/s)	Δ_{Eq2} (mm/s)	$\delta_{(av)}$ (mm/s)	$\Delta_{Eq(av)}$ (mm/s)
I	0.46	0.95	0.37	0.76	0.43	0.82
	0.48[b]	1.38[b]	0.35[b]	−0.62[b]		
II	0.50	1.26	0.39	0.72	0.46	
	0.48[c]	1.58[c]	0.34[c]	0.73[c]		
	0.47[c]	1.30[c]				
III	0.50	0.79	0.47	0.61	0.49	0.67
IV					0.41	0.99
V					0.43	0.70
VI	0.48	0.78	0.40	0.62	0.45	
	0.67					

[a] δ_1 and δ_2 values are based on the 2:1 fitting of the spectral profile. $\delta_{(av)}$ is the average isomer shift of δ_1 and δ_2. [b] Values obtained at 4.2 K. [c] Values obtained at 4.2 K by a fit using three Fe sites.

zero-valent molybdenum. The CO stretching vibrations in I are observed at 1868 and 1750 cm^{-1}, which are also consistent with the presence of Mo(0).

The average Moessbauer parameters of the complexes I–VI show some dependence of the isomer shift (IS) on the nature of the terminal ligand on the iron site. The data in Table III show that complexes with terminal ligands such as Cl, OPh, SEt, and SBz have average IS values of ca. 0.40 mm/s and Δ_{Eq} values of ca. 0.85 mm/s. However, when the terminal ligand at the iron site is SC_6H_5-*p*-OMe, IS and Δ_{Eq} values of 0.49 and 0.67 mm/s, respectively, are obtained. Apparently the sulfur atom in the SC_6H_5-*p*-OMe ligand (especially with the electron releasing OMe-*p*-substituent) interacts with the π system of the aromatic ring and donates more electron density to the iron atom. As a result, the isomer shift value is larger in magnitude than in the case of a sulfur that is bound to an aliphatic chain. Similar differences in the isomer shift values that are attributed to differences in the type of the terminal ligand have already been observed for analogous clusters such as $[MoFe_3S_4]^{2+}$,[39] $[Fe_4S_4L_4]^{2-}$,[40] and $[Fe_2S_2L_4]^{2-}$.[41] The electronic effects that affect the IS values of the complexes I–VI also show their expected influence in other spectroscopic as well as electrochemical characteristics. The Moessbauer spectrum of the $[W(CO)_3Fe_3S_4(SPh\text{-}p\text{-}OMe)_3]^{3-}$ cluster V, shows a broad quadrupole doublet with an isomer shift (IS) of 0.43 mm/s and a quadrupole splitting (Δ_{Eq}) of 0.70 mm/s. This value of isomer shift is lower in magnitude than the isomer shift value observed for the molybdenum analogue $[Mo(CO)_3Fe_3S_4(SPh\text{-}p\text{-}OMe)_3]^{3-}$. The slight differences in the Moessbauer parameters between the molybdenum and tungsten clusters are as expected and have already been noted in other similar clusters.[15]

Detailed temperature and applied magnetic field studies of the Moessbauer spectra of the $[Mo(CO)_3Fe_3S_4(SR)_3]^{3-}$ complexes were undertaken to establish certain basic details of electronic structure. Moessbauer spectra of the complexes I and III (R = Et, Bz) have been obtained at 4.2 K in applied magnetic fields up to 6.0 T and at zero field for higher temperatures up to 250 K.

The zero field spectrum at 4.2 K for the anion with R = Et is shown in Figure 3A. The high velocity line shows clearly the presence of two components with unequal intensities. As indicated above the structural data suggest the presence of two iron species with an intensity ratio of 2:1. However, attempts to fit the spectra with two quadrupole doublets with an area ratio of 2:1 do not give satisfactory results. It was found necessary to include a third doublet with Moessbauer parameters δ = 0.44 mm/s and Δ_{Eq} = 0.93 mm/s which represents about 15% of the total area. We attribute this component to an impurity anion species which depends on the preparation conditions. This assumption was substantiated by measurements on a sample from a different preparation where this component was more pronounced, allowing a more reliable determination of the Moessbauer parameters. The values of the hyperfine parameters suggest that the impurity species is an $[Fe_4S_4]^{2+}$ species with an S = 0 ground state. This would give a diamagnetic component in applied field spectra, as indeed is observed (vide infra and footnote b in Table II).

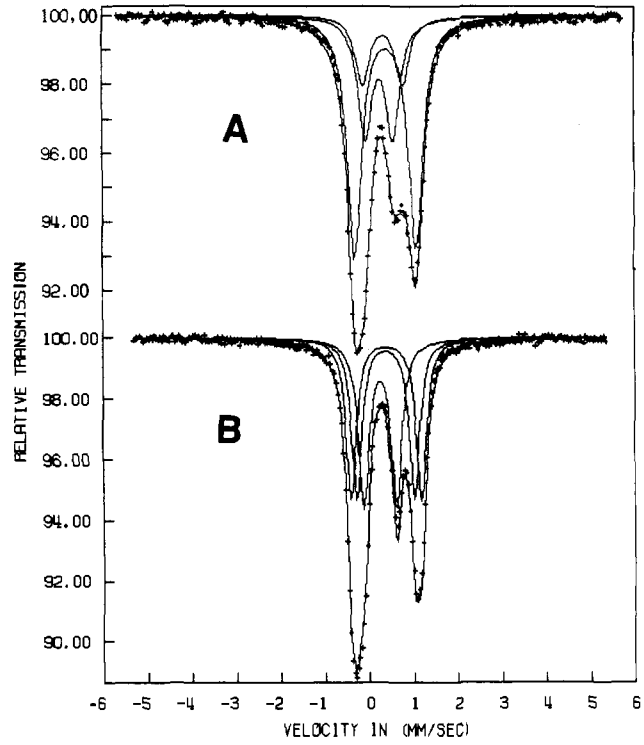

Figure 3. Moessbauer spectra of crystalline powders of $(Et_4N)_3[Fe_3S_4(RS)_3Mo(CO)_3]$ at 4.2 K in zero applied magnetic field (A) for R = Et and (B) for R = Bz). The parameters of the components shown by the solid lines are given in Table IV. The spectrum of R = Et contains the contribution of an impurity (see text).

The zero field spectrum at 4.2 K for the anion with R = Bz is shown in Figure 3B. In this case, the high velocity line shows clear resolution in at least two components, and satisfactory fits could be obtained with two quadrupole doublets with an area ratio of 2:1. On the basis of this analysis the more intense doublet exhibits a line width higher than the instrumental line width indicating that the two Fe atoms giving rise to it may be slightly different. This observation suggests that the 4.2 K zero field spectrum can be analyzed with three quadrupole doublets of equal intensity. The spectrum was fitted to three doublets with 1:1:1 area ratio, and the resulting hyperfine parameters are listed in Table IV.

Before proceeding further, it is useful to summarize the results from the zero field spectra at 4.2 K for the R = Et, Bz complexes. In both cases the spectrum of the major doublet, of the two

(39) Mascharak, P. K.; Armstrong, W. H.; Mizobe, Y.; Holm, R. H. *J. Am. Chem. Soc.* **1983**, *105*, 475.
(40) Kanatzidis, M. G.; Coucouvanis, D.; Simopoulos, A.; Kostikas, A.; Papaefthmiou, V. *J. Am. Chem. Soc.* **1985**, *107*, 4925.
(41) Salifoglou, A.; Simopoulos, A.; Kostikas, A.; Dunham, W. R.; Kanatzidis, M. G.; Coucouvanis, D. *Inorg. Chem.* **1988**, *27*, 3394.

Table IV. Fine and Hyperfine ^{57}Fe Moessbauer Parameters[a] for the Cluster Anions $[Fe_3S_4(SEt)_3Mo(CO)_3]^{3-}$ (I) and $[Fe_3S_4(SBz)_3Mo(CO)_3]^{3-}$ (II) and Comparison with Protein Bound and Other Similar Centers

center	site	δ[a] (mm/s)	Δ_{Eq} (mm/s)	η	β	A_x (KG)	A_y (KG)	A_z (KG)	A (KG)	D (cm^{-1})	E/D
I	I	0.48 (1)[b]	1.38 (2)	0.95 (10)	30 (5)	−110 (20)	−150 (10)	−110 (5)	−123	−3.0	0.25
	II	0.35	−0.62	−2.0	50	+100	+115	+118	+111		
II	Ia	0.48	1.58	0.95	25	−110	−180	−109	−133		
	Ib	0.47	1.30	0.95	25	−110	−180	−104	−131	−3.0	0.25
	II	0.34	0.73	1.0	70	+100	+115	+120	+112		
A[c]	I	0.46	1.47	0.4	20	−150	−150	−120	−140	−2.5	0.23
	II	0.32	−0.52	−2.0	16	+100	+115	+126	+114		
B[d]	Ia	0.49	1.46		25	−139	−139	−110	−129	−2.5	0.25
	Ib	0.46	1.15		15	−139	−139	−117	+123		
	II	0.31	0.56		50	+124	+124	+120	−118		
C[e]	Ia	0.47	0.49	0	30	−135	−110	−110	−118	−2.8	0.31
	Ib	0.46	1.21	0	20	−135	−110	−110	−118		
	II	0.34	−0.59	2.5	0	+80	+110	+124	+105		

[a] With respect to Fe metal at room temperature. [b] Numbers in parentheses are estimated errors in the last decimal figure. [c] A = Fe_3S_4 center in *D. gigas* Fd II, ref 42. [d] B = Fe_3S_4 center in aconitase, ref 44. [e] C = $Fe_4S_4(LS_3)(t\text{-BuNCO})_3]^{1-}$, ref 23.

observed in a 2:1 ratio, has parameters indicative of a $Fe^{2.5}$ oxidation state. This suggests that an electron is shared equally by the two irons in this site (site I in Table IV). The parameters of the minority doublet are typical of Fe^{3+}. These results are remarkably similar to those obtained from *D. gigas* ferredoxin II and can be interpreted as arising from the cubane-type fragment $[Fe_3S_4Mo(CO)_3]^0$ containing a delocalized Fe^{2+}–Fe^{3+} pair, a single Fe^{3+} site, and a unique hexacoordinated Mo fourth site which has $S = 0$ and thus is not spin coupled to the remaining Fe_3S_4 cluster fragment. This situation is analogous to the recently studied similar anion $[Fe_4S_4(LS_3)(t\text{-BuNC})_3]^{1-}$[23] where, however, the unique subsite is occupied by a low spin Fe^{2+} species which complicates the Moessbauer spectra.

The magnetically perturbed Moessbauer spectra confirm and give further details on the spin coupling in the Fe_3S_4 fragment. Spectra of the cluster with R = Et recorded in transverse applied magnetic fields of 4.0 and 6.0 T are shown in Figure 4 (parts A and B, respectively). The experimental spectra in Figure 4 were obtained by subtracting from the raw data 15% of a theoretical diamagnetic spectrum of the impurity identified in the zero field spectra at 4.2 K. Comparison of the two spectra in Figure 4 shows two sets of lines, one moving outward with increasing field and the other inward. This indicates the presence of two components arising from two antiferromagnetically coupled sites corresponding to the Fe^{2+}–Fe^{3+} pair (site I) and the single Fe^{3+} (site II). Again the similarity to corresponding spectra of Fd II is striking. In view of this we have performed computer simulations using an electronic spin Hamiltonian with $S = 2$ and the methodology of spectral analysis described in detail earlier.[42,43] We have applied this model with an area ratio of 2:1 for the two components using as a starting set the hyperfine parameters of Fd II. The results of the spectral simulations are presented in Figure 4 (parts A and B); the latter shows a decomposition of the 6.0 T spectrum into the spectra of the two sites. The final parameter set used is listed in Table IV.

The 4.2 K magnetically perturbed spectra of the complex with R = Bz exhibit very similar patterns as in the case of R = Et with a slight complication in the analysis due to the inequivalence between the sites of the delocalized pair. Similar inequivalences were found in studies of the Fe_3S_4 center of aconitase[44] and in the synthetic cluster reported by Weigel et al.[23] The experimental spectra in applied transverse magnetic fields are shown in Figure 5 (parts A and B). By following a procedure similar to that used for the cluster with R = Et we have determined the set of fine and hyperfine parameters listed in Table IV. The solid lines in Figure 5 (parts A and B) are theoretical curves calculated with the parameters of Table IV. A spectral decomposition into the

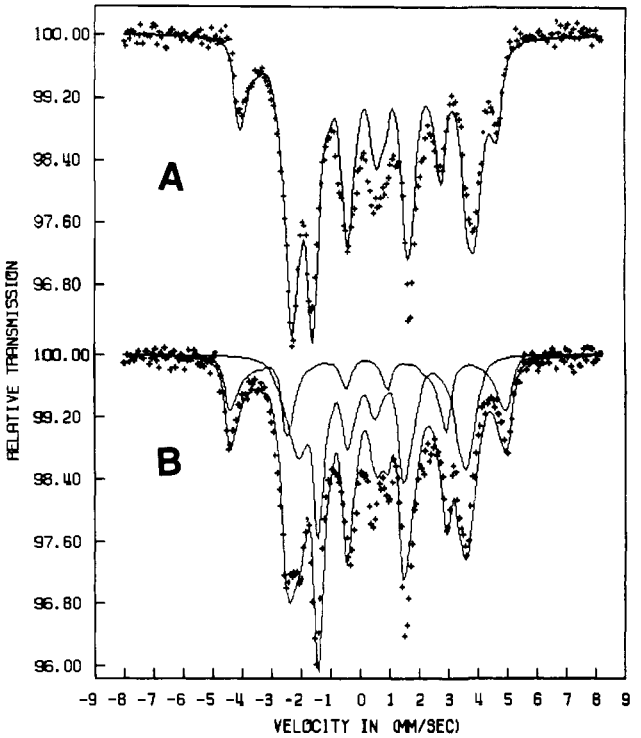

Figure 4. Moessbauer spectra of crystalline powders of $(Et_4N)_3[Fe_3S_4(EtS)_3Mo(CO)_3]$ at 4.2 K in an applied transverse magnetic field of 4.0 T (A) and 6.0 T (B). Calculated spectra with the spin coupling model described in the text are shown by the solid lines. The decomposition of the 6.0 T spectrum into two components corresponding to the delocalized Fe^{2+}–Fe^{3+} pair and the single Fe^{3+} site is shown in (B). The increase of the magnetic splitting of one component and the decrease of the other demonstrates that the two components are antiferromagnetically coupled.

contribution of the Fe^{3+} (site II) and the delocalized pair (sites Ia and Ib) is shown in Figure 5B. No further decomposition of the delocalized pair is shown since the two subcomponents are very similar and would only worsen the clarity of the figure. Considerable misfit is observed in this central region of the spectrum. Since the zero field spectra do not give any indication of an impurity contribution, we attribute this misfit to texture effects.

For comparison we have included in Table IV the fine and hyperfine parameters determined from Moessbauer studies of *D. gigas* Fd II,[42] aconitase,[44] and the synthetic cluster $[Fe_4S_4(LS_3)(t\text{-BuNC})_3]^{1-}$.[23] The data of this table offer unequivocal evidence that the ground state electronic properties of all the systems listed are identical within the experimental errors. The structural data for the complexes of the present study demonstrate that the anions can be considered as consisting of a $[Fe_3S_4]^0$ core weakly coupled to the Mo $S = 0$ moiety. We can therefore

(42) Papaefthymiou, V.; Girerd, J. J.; Moura, I.; Moura, J. J. G.; Munck, E. *J. Am. Chem. Soc.* **1987**, *109*, 4703.
(43) Papaefthymiou, V.; Simopoulos, A.; Kostikas, A.; Coucouvanis, D. *Hyperf. Inter.* **1986**, *30*, 337.
(44) Surerus, K. K.; Kennedy, M. C.; Beinet, H.; Munck, E. *Proc. Natl. Acad. Sci. U.S.A.* **1989**, *86*, 9848.

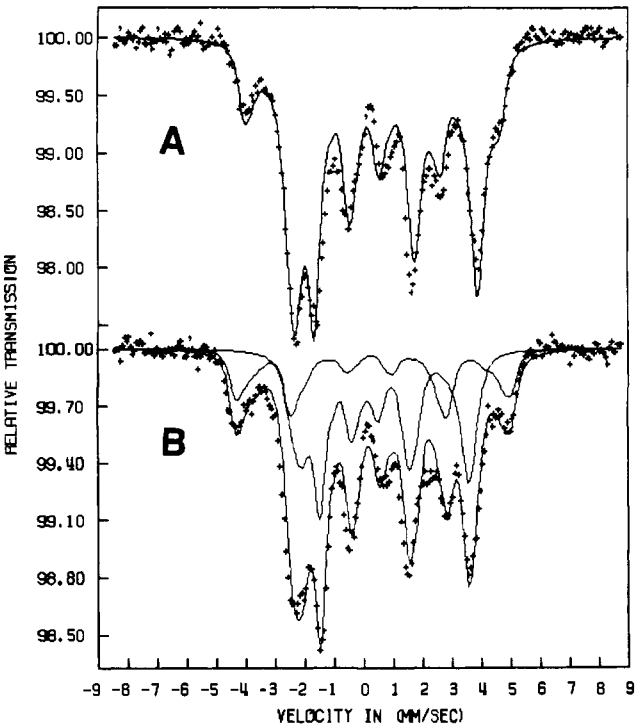

Figure 5. Moessbauer spectra of crystalline powders $(Et_4N)_3[Fe_3S_4(BzS)_3Mo(CO)_3]$ at 4.2 K in an applied transverse magnetic field of 4.0 T (A) and 6.0 T (B). Calculated spectra with the spin coupling model described in the text are shown by the solid lines.

conclude that the parameters of Table IV characterize the ground state of this cluster both in the synthetic complexes and in protein-bound centers. *The most interesting feature of the electronic ground state, unambiguously demonstrated by the Moessbauer data, is the presence of a delocalized pair of Fe^{3+}–Fe^{2-} ferromagnetically coupled to give $S_{12} = {}^9/_2$ which combines antiferromagnetically with the spin $S = {}^5/_2$ of the remaining Fe^{3+} ion to give the total spin $S = 2$ of the cluster.*

The zero field spectra show strong temperature dependence in the temperature region of 4.2–200 K. At >200 K we observe only one symmetric doublet for the R = Et compound and one asymmetric doublet for the R = Bz. The values of isomer shift and quadrupole splitting correspond closely to the mean values of sites I and II at 4.2 K corrected for second order Doppler shift. This behavior may be attributed to a strong temperature dependence of Δ_{Eq} for the delocalized pair and/or to the contribution of a completely delocalized state of the extra electron over the three iron sites. The previous application of both models to similar results of temperature dependence in the case of Fd II has led to the suggestion that the second cause is the most probable. Nevertheless, the known, sensitive temperature dependence of Δ_{Eq} in Fe_4S_4 clusters, on the type and orientation of terminal ligands,[45] suggests that additional detailed studies of temperature dependence are required to resolve this question.

Summary and Conclusions

The new class of single cubane $[M(CO)_3Fe_3S_4L_3]^{3-}$, (M = Mo, W; and L = Cl, SEt, SBz, OPh, and SC_6H_4-*p*-OMe) clusters prepared in this work represent a new entry to the Fe/Mo/S clusters. These complexes are formed by an internal, reductive reorganization of the linear $[Fe_3S_4L_4]^{3-}$ complexes on a $M(CO)_3$ template, M = Mo and W. The most important chemical characteristic of the $[Mo(CO)_3Fe_3S_4L_3]^{3-}$ clusters is their tendency to undergo core reactions and conversions. The octanuclear $[Fe_6S_6(L)_6\{Mo(CO)_3\}_2]^{n-}$ clusters, with a dodecahedral core structure, are obtained thermally through loss of S^{2-} and structural transformation of the $[MFe_3S_4]^0$ core clusters. When the terminal ligand L on the iron site is Cl or OPh, this transformation proceeds upon warming solutions of the cubic clusters to 50 °C for ca. 30 min. However, when the ligand is OC_6H_4-*p*-COMe, the transformation proceeds at room temperature.

Various chemical and structural transformations of the $[MFe_3S_4]^0$ core also are observed upon oxidation with various oxidizing agents. The reaction of the $[Mo(CO)_3Fe_3S_4(SR)_3]^{3-}$ clusters with organic disulfides results in the oxidation of the molybdenum atom and the formation of the triply-bridged double-cubane $[Mo_2Fe_6S_8(SR)_9]^{3-}$ clusters. In this reaction, the $[MFe_3S_4]^0$ core does not undergo severe structural changes; however, the product contains the $Mo_2(\mu^2\text{-}SR)_3$ structural unit that is formed by the coupling of two $[Mo(SR)_xFe_3S_4(SR)_3]^{3-}$ units. The triply-bridged double cubane has previously been obtained only by the spontaneous self-assembly reaction.[33]

Simple oxidative decarbonylation of the molybdenum site is observed when the $[Mo(CO)_3Fe_3S_4Cl_3]^{3-}$ cluster is oxidized with quinone. The product from this reaction is the solvated single cubane $[Mo(cat)(MeCN))Fe_3S_4Cl_3]^{2-}$. In contrast, when $[Mo(CO)_3Fe_3S_4(SR)_3]^{3-}$ is oxidized with quinone, the doubly-bridged double-cubane $[(Mo(cat))_2Fe_6S_8(SR)_6]^{4-}$ is obtained.

The unique core conversions and reactions that are observed with the $[MFe_3S_4]^0$ core (Figure 2) are of great interest in the synthetic chemistry of the Fe/Mo/S clusters and demonstrate the utility of this unit as a synthetically versatile starting material.

The clusters that contain the $[MFe_3S_4]^0$ core are best described as weak complexes of the diamagnetic $M(CO)_3$ moiety with the cubic Fe_3S_4 "ligand" unit. The latter appears to be structurally, electronically, and magnetically nearly identical to the reduced $[Fe_3S_4]$ center of the iron-sulfur proteins of *A. vinelandii* Fd II and *D. gigas*. The oxidized form of the clusters, $[M(CO)_3Fe_3S_4L_3]^{2-}$, is characterized[21] by a spin ground state of $S = {}^3/_2$. In contrast, the oxidized form of the three-iron protein $[Fe_3S_4]$ centers is characterized by an $S = {}^1/_2$ ground state. In the reduced form the $[M(CO)_3Fe_3S_4L_3]^{3-}$ complexes are EPR silent and possess an integer spin state. The reduced form of the three-iron center in Fe/S proteins are also EPR silent.

The major difference between the $[MoFe_3S_4]^0$ and $[MoFe_3S_4]^{3+}$ cores is that the $[MoFe_3S_4]^0$ core contains molybdenum in the zero oxidation state, while the $[MoFe_3S_4]^{3+}$ core formally contains molybdenum(III). The electrochemical studies on the $[MoFe_3S_4]^0$ core establish the three-membered electron transfer series that are described in terms of three hitherto unknown $[MoFe_3S_4]$ oxidation levels.

$$[MoFe_3S_4]^{1+} \rightarrow [MoFe_3S_4]^0 \rightarrow [MoFe_3S_4]^{1-}$$

In the $[MoFe_3S_4]^{3+}$ core, electrochemical studies already have established the three-membered electron transfer series that are obtained mainly with π donor ligands coordinated to the Mo atom.

$$[MoFe_3S_4]^{2+} \rightarrow [MoFe_3S_4]^{3+} \rightarrow [MoFe_3S_4]^{4+}$$

It appears that, depending on the type of terminal ligands (π donors vs π acceptors) involved, the number of distinct oxidation levels that the $[MoFe_3S_4]$ core can span is six, and the most reduced forms, not unexpectedly, are only stable with π acceptor ligands. Changes in the oxidation levels of the $[MoFe_3S_4]$ cores are accompanied by changes in the electronic and magnetic structures. Both the $[MoFe_3S_4]^0$ and $[MoFe_3S_4]^{2+}$ cores are EPR silent, while the $[MoFe_3S_4]^{1+}$ and $[MoFe_3S_4]^{3+}$ cores are EPR active and exhibit spectra that correspond to $S = {}^3/_2$ spin ground states.

As stated previously, the conversion of the $[MoFe_3S_4]^0$ core to the $[MoFe_3S_4]^{3+}$ core is accomplished by the irreversible oxidative decarbonylation of the former with Cl_4-1,2-benzoquinone. The importance of this reaction is that it connects the two cores electronically and chemically. Whether the reverse reaction, and reduction of the $[MoFe_3S_4]^{3+}$ core to $[MoFe_3S_4]^0$, promotes the introduction of π acceptor ligands to the coordination sphere of the Mo atom (by substitution of π donor ligands) remains to be established. If this were the case, however, it would provide a possible pathway for the entry of N_2 to the Mo site of clusters that contain the $[MoFe_3S_4]^0$ cores. Such an event has been

(45) Frankel, R. B.; Averill, B. A.; Holm, R. H. *J. Phys. (Paris)* **1974**, *35*, C6.

advanced previously[46] as a necessary step in a proposed pathway for the activation and reduction of N_2 with a nitrogenase active site model that employs S^{2-} bridged $[MoFe_3S_4]$ and $[Fe_4S_4]$ centers.

Acknowledgment. The support of this work by a grant (GM-33080) from the National Institutes of Health is gratefully acknowledged.

(46) Coucouvanis, D. *Acc. Chem. Res.* **1991**, *24*, 1-8.

Supplementary Material Available: Tables of positional parameters, thermal parameters, and selected distances and angles for $(Et_4N)_3[Fe_3S_4(SEt)_3Mo(CO)_3]\cdot CH_3CN$ (**I**) (7 pages); table of observed and calculated structure factors for I (6 pages). Ordering information is given on any current masthead page. The same crystallographic data for I have been deposited with a previous communication[21] and can be obtained on request from the Fachinformationzentrum Energie, Physik, Mathematik GmbH, D-7514 Eggenstein-Leopoldshafen 2 (FRG), on quoting the depository number CSD-53196, the names of the authors, and the journal citation.

Mechanism of Aromatic Hydroxylation in a Copper Monooxygenase Model System. 1,2-Methyl Migrations and the NIH Shift in Copper Chemistry

M. Sarwar Nasir, Brett I. Cohen, and Kenneth D. Karlin*

Contribution from the Departments of Chemistry, The Johns Hopkins University, Baltimore, Maryland 21218, and State University of New York at Albany, Albany, New York 12222.
Received September 11, 1991

Abstract: The NIH shift mechanism appears to be operative in a copper monooxygenase model system involving dicopper ion complex mediated O_2 hydroxylation of an arene substrate. Previous studies have shown that when a dicopper(I) complex containing two tridentate PY2 units (PY2 = bis[2-(2-pyridyl)ethyl]amine) which are linked by a *m*-xylyl group, i.e., $[Cu_2(XYL\text{-}H)]^{2+}$ (**1**), is reacted with dioxygen, a Cu_2O_2 intermediate forms and hydroxylation in the intervening 2-xylyl position occurs. Here, corresponding reactions of 2-methyl substituted analogues $[Cu_2(Me_2XYL\text{-}CH_3)]^{2+}$ (**4**) and $[Cu_2(XYL\text{-}CH_3)]^{2+}$ (**5**) are described in detail. Oxygenation of these causes xylyl hydroxylation reactions producing new phenol products, with concomitant 1,2-migration of the methyl group, loss of one PY2 ligand arm, and formaldehyde formation. Manometric O_2 uptake experiments and an $^{18}O_2$ labeling study confirm that the stoichiometry of these reactions are consistent with that observed for monooxygenases. A reaction carried out using a dinucleating ligand which has been deuterated in benzylic positions confirms that the CH_2O product is derived from this carbon atom, a result also consistent with migration of the 2-methyl group. A small yield of methylbis[2-(2-pyridyl)ethyl]amine (MePY2) is consistently obtained, and experiments suggest this may be derived from the reduction of an intermediate iminium salt $\{CH_2{=}N[CH_2CH_2PY]_2\}^+$ (PY = 2-pyridyl). The hydroxylation induced 1,2-methyl migrations observed here are reminiscent of the NIH shift reactions previously observed only in iron hydroxylases and suggest that the copper ion mediated reactions proceed by the electrophilic attack of a Cu_2O_2 intermediate upon the proximate aromatic substrate. A detailed mechanism is proposed and discussed in terms of the known O_2 reactivity and structure of these dinuclear copper complexes. The biological relevance and significance of this monooxygenase model system is also discussed.

Introduction

Widely occurring copper enzymes are involved in the processing or utilization of dioxygen.[1-3] Functions performed include O_2 transport by hemocyanin (Hc),[4] substrate mono- and dioxygenation, and oxidation (dehydrogenation) of substrates with concomitant reduction of O_2 to either H_2O_2 or water (e.g., oxidases). Monooxygenases of copper have attracted a great deal of recent attention, along with iron enzymes such as (i) cytochrome P-450 monooxygenase,[5] (ii) non-heme iron methane monooxygenase (MMO),[6] and (iii) pterin-dependent phenylalanine hydroxylase.[7] This is due to the importance of the reactions they catalyze, an interest in the fundamental chemistry involved, and the hope to mimic the mild and selective biological oxygenation reactions in model systems or in synthetically useful applications. Copper monooxygenases[8-12] include tyrosinase (Tyr; *o*-phenol hydroxylase),[8] pterin-dependent *Chromobacterium violaceum* phenylalanine hydroxylase (PAH),[7,9] dopamine β-hydroxylase (benzylic hydroxylation of dopamine yielding the neurotransmitter norepinephrine),[10] and peptidylglycine α-amidating monooxygenase[11] (PAM; oxidative N-dealkylation of glycine-extended neuropeptide prohormones).

Tyr and Cu-dependent PAH effect aromatic hydroxylation reactions, which undoubtedly occur via different mechanisms since

* Author to whom correspondence should be addressed at the Department of Chemistry, The Johns Hopkins University, Charles & 34th Streets, Baltimore, MD 21218.

(1) (a) Karlin, K. D.; Gultneh, Y. *Prog. Inorg. Chem.* **1987**, *35*, 219-327. (b) *Copper Proteins and Copper Enzymes*; Lontie, R., Ed.; CRC: Boca Raton, FL, 1984; Vol.s 1-3. (c) *Metal Ion Activation of Dioxygen: Metal Ions in Biology*; Spiro, T. G., Ed.; Wiley-Interscience: New York, 1981; Vol. 3.

(2) Sorrell, T. N. *Tetrahedron* **1989**, *45*, 3-68.

(3) Tyeklár, Z.; Karlin, K. D. *Acc. Chem. Res.* **1989**, *22*, 241-248.

(4) (a) Volbeda, A.; Hol, W. G. J. *J. Mol. Biol.* **1989**, *209*, 249-279. (b) Solomon, E. I. In *Metal Clusters in Proteins*; Que, L., Jr., Ed.; ACS Symposium Series 372; American Chemical Society: Washington, DC, 1988; pp 116-150.

(5) (a) Dawson, J. H. *Science* **1988**, *240*, 433-439, and references cited therein. (b) *Cytochrome P-450*; Ortiz de Montellano, P. R., Ed.; Plenum: New York, 1986.

(6) Que, L., Jr.; True, A. E. *Prog. Inorg. Chem.* **1991**, *38*, 97-200.

(7) Dix, T. A.; Benkovic, S. J. *Acc. Chem. Res.* **1988**, *21*, 101-107.

(8) (a) Wilcox, D. E.; Porras, A. G.; Hwang, Y. T.; Lerch, K.; Winkler, M. E.; Solomon, E. I. *J. Am. Chem. Soc.* **1985**, *107*, 4015-4027. (b) Robb, D. A. In *Copper Proteins and Copper Enzymes*; Lontie, R., Ed.; CRC: Boca Raton, FL, 1984; Vol. 2, pp 207-241. (c) Lerch, K. *Met. Ions Biol. Syst.* **1981**, *13*, 143-186.

(9) Pember, S. O.; Johnson, K. A.; Villafranca, J. J.; Benkovic, S. J. *Biochemistry* **1989**, *28*, 2124-2130.

(10) (a) Brenner, M. C.; Klinman, J. P. *Biochemistry* **1989**, *28*, 4664-4670. (b) Stewart, L. C.; Klinman, J. P. *Ann. Rev. Biochem.* **1988**, *57*, 551-592.

0002-7863/92/1514-2482$03.00/0